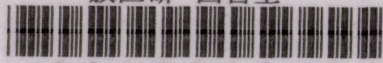
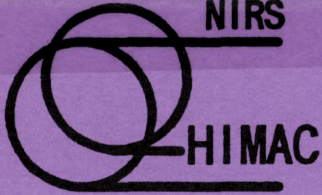


放医研 図書室



8 0 1 9 9 6 0 1 4

NIRS



HIMAC

NIRS-M-111
HIMAC-011

Analysis of the Ripple Current in the HIMAC Synchrotron

Masayuki KUMADA

January 1996



National Institute of Radiological Sciences

4-9-1, Anagawa, Inage-ku, Chiba 263 JAPAN

Analysis of the Ripple Current in the HIMAC Synchrotron

Masayuki Kumada
National Institute of Radiological Sciences
4-9-1 Anagawa, Inage, Chiba, Japan
(e-mail) kumada@nirs.go.jp

Abstract

Ripple content of the HIMAC synchrotron is below ppm level at rated excitation. This performance is mainly due to taking the measures of the common mode ripple and spike by the bridge resistor, the separate connection of the coil and the mode filter system. In presence of the common mode, where the ground line plays an essential role, the circuit is described by the three inputs and three outputs and is not easy to evaluate in this form. A mode separation is possible in case of a symmetric configuration with respect to the ground line. By the mode separation, this circuit can be reduced to a decoupled circuit of the normal mode and the common mode of two inputs and two outputs. With this decoupling, simple formulae are derived both in the frequency domain for the analysis of the ripple and in the time domain for the analysis of the spike current. This analysis forms the bases of the understanding of the low ripple performance.

I. Introduction

HIMAC synchrotron is stable and reproducible. Since the commissioning, the power supply of the HIMAC shows low ripple contents[1] and has been improved by an order of magnitude by now[2]. In particular, ripple content at the flat top of the trapezoidal current is small. Relative ripple current of the Bending magnet power supply and the Focussing Quadrupole magnet power supply is 0.2 to 0.3 ppm in RMS when they are normalized by the rated full current [2,3], which are estimated from the calculation of the voltage ripple and the admittance of the load. Admittance is measured and calculated based on the model of the six terminal ladder circuit. High performance is due to new approaches taken in the HIMAC synchrotron which are,

(i) mode concept of the normal and common both in the power supply and

the load,

(ii) analytical formulation for the mode analysis,

(iii) finding of a performance limiting factor in existing synchrotrons and finding appropriate means against it,

(iv) finding of the resonance between the power supply and the load in the modes and taking appropriate measures.

We started from the proposition that the load of the synchrotron power supply is a ladder circuit where it is a cascaded circuit of a repeated cell of the LCR element. Ladder circuit is originally introduced in the CPS design[4] by Regenstreif and later in the SPS[5] by Van Der Meer as a transmission line circuit. Characteristic feature of this ladder circuit is the capacitances between the excitation coil and the iron yoke of the magnet. Iron yokes are at the earth potential, and the ladder circuit forms the six terminal circuit of three inputs and three outputs[6,7,8]. In the HIMAC, the ground line is running along the ring with the power line so that the load is modeled by the six terminal circuit without ambiguity. In this model, the outgoing current I from the power supply is not identical to the incoming current J from the load, which contrasts with the existing transmission line type models [9,10,11,12,13,14,15]. Difference current $I-J$ flows through the ground line. When one defines the voltage from the ground line to the positive power line as U , and the voltage from the negative power line to the ground line as V , one can define two sets of voltage and current, namely $U+V$, $I+J$, $U-V$ and $I-J$. Former set is the normal mode and the latter set is the common mode. Analysis of this six terminal circuit has not been done in the past. A computer simulation was avoided as it is time consuming and it has a shortcoming of grasping a physical image of the problem. It was found that in general the mode separation is possible by eigenvalue problem method. In particular, when the elements connected to the positive power line and the elements connected to the negative power line are located identically, it can be shown that the normal mode and common mode are decoupled. Owing to the finding of this mode decoupling, the model of six terminal circuit can be treated as the four terminal circuit and the standard theory can be applied [16]. Decoupled formulation is simple yet powerful to fully describe the resonant property of the ladder circuit of both the normal and the common modes, and the most of the quantities can be expressed by simple closed expressions with variables of complex number. The author found the analytic solution in the time domain by inverse Laplace transform by

decomposing into a partial fractional expression or equivalently by using the Heaviside theorem. Spike is described as a transient response of the ladder circuit. This analytical treatment helps to understand the nature of the ladder circuit. To verify the validity of the present model, the frequency characteristic of the admittance of the magnet string was measured and was confirmed to be valid[2]. The resonance is observed in the admittance.

Three major actions are taken to cope with the resonance:

(i) Bridge resistors were connected across the coil in parallel to damp the resonance. In the time domain, this resistor changes oscillatory spike to exponentially decaying spike whose width is shortened. This resistor also works to reduce logical ripples whose frequencies are beyond 1200 Hz by bypassing the current.

(ii) Upper and the lower coils are separately connected to realize higher symmetric configuration. In separate connection, the common mode currents of opposite sign generate canceled magnetic field. when the hardware is not perfectly made the normal mode and the common mode mixes. Every hardware can not be made perfect. Mode decoupling is not perfect and the measure against the common mode is preferable.

(iii) Common mode static filter is added. This filter is of great help to reduce the common mode ripple beyond the fundamental logical ripple.

In this way, from the very beginning of the commissioning, the HIMAC synchrotron is free from the logical ripple and spike except the ripple frequencies of 50 Hz and 100 Hz[1,2]. 50 Hz and 100 Hz ripples are the frequencies of illogical ripple that cannot be reduced by the static filter, by the bridge resistor. Active filter suppresses the 100 Hz ripple. 50 Hz ripple could be reduced by replacement of DCCT by other DCCT of better performance[2]. Final ripple content of the focusing Quadrupole and Bending magnet was well below ppm level[2]. In the following, the analysis of the HIMAC synchrotron is presented.

II. Mode Analysis of the Ladder Circuit

Excitation coils of the magnet string are divided into upper and lower coil for the Bending magnet and Quadrupole magnet as shown in Figure1. For the Quadrupole magnet with four poles, there are several ways of combinations to separate them into two parts. The upper and lower coils of the HIMAC Quadrupole are grouped separately from a view point of simple connection.

It is possible and better to group the coils of north poles(N) and south poles(S) although the way of the connection is more complicated. Impedance of the common mode depends on the way how they are connected. The common mode impedance of grouping into N-N poles and S-S poles in Quadrupole is much smaller than the inductance of upper and lower coils as the flux due to the common mode voltage cancels each other. In the HIMAC Bending magnet, the common mode impedance is less than one percent of that of the normal mode and in the Quadrupole magnet it is half of the normal mode.

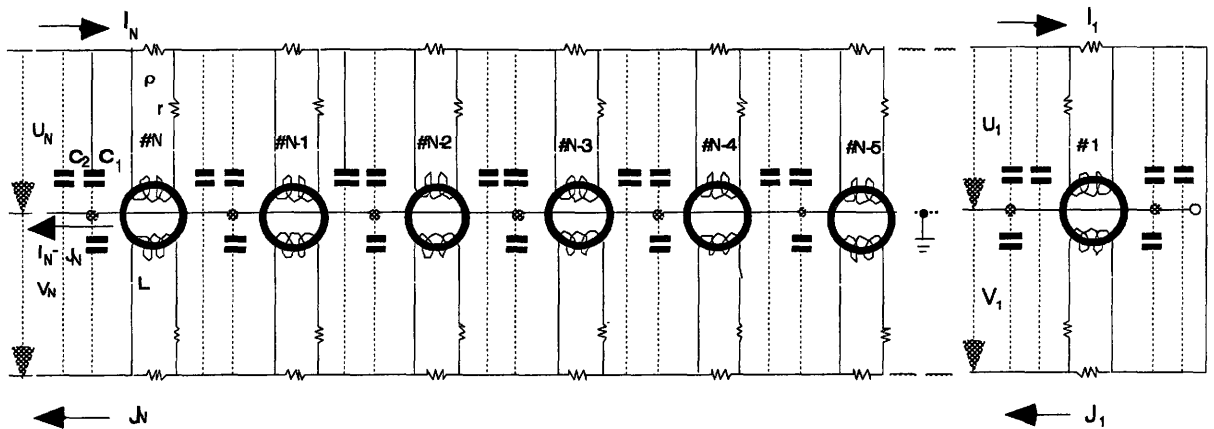


FIGURE 1. Equivalent circuit of the HIMAC six terminal ladder circuit. The upper and lower coils are magnetically coupled through magnet yoke. $N=12$ for Quadrupole magnet and $N=13$ for Bending magnet. The solid line represents the real physical line and the dotted line represents the line of stray capacitance.

A unit of magnet with a stray capacitance can be represented by a six terminal circuit of three inputs and three outputs. For the ease of the analysis, this unit cell is treated as π type cell. Voltage across the earth and the upper coil and the voltage across the lower coil to the earth of the n -th cell is designated as U_n and V_n with a suffix n , where n represents the location of the cell counted from the end of the magnet as shown in Figure 1. Cable currents flowing in the upper coil (the P line) and the lower coil (the N line) are designated as I_n and J_n . Elements of "symmetric" nature such as magnet, reactor and capacitor with respect to the ground line leads to a separation of a coupled mode into decoupled mode to a first order approximation. They are the normal mode and the common mode. The normal mode is designated as (U_n+V_n) and (I_n+J_n) and the common mode is designated as (U_n-V_n) and (I_n-J_n) . Although mathematically, the mode

separation is possible even for the asymmetric circuit by finding an eigenvalue and an eigenvector, a symmetric circuit is much easier to handle and to find a remedy for suppressing harmful ripple and spike.

Mode separation enables us to treat the six terminal circuit into well known four terminal circuit. A relation of the input and the output voltages and those of the currents are expressed by two by two transfer matrixes for the decoupled four terminal circuit. Expressing the elements of the matrix by hyperbolic sinusoidal function, one can use de Moivre theorem for repeated cells. In reality, the symmetry assumed is not perfect and is broken to some extent due to an imbalance of the capacitances or the inductances of the upper and the lower coils. This asymmetry causes the mode mixing.

End of the normal mode circuit, where the main excitation current of the magnet flows, is shorted. Several choices of the termination at the end for the common mode are possible namely, open, short and termination with impedance. We chose an open-ended condition for the HIMAC.

Primary objective of this analysis is to derive simple expressions of the normal and common mode to make an evaluation of the ripple and the spike current in the HIMAC. The mode admittance of the ladder circuit is expressed by a product of the characteristic admittance Y_{op} , which is an inverse of the characteristic impedance Z_{op} defined by the eq.(2-34) and (2-35), and a hyperbolic sinusoidal function where the subscript $p=n$ stands for the normal mode and the $p=c$ stands for the common mode. The following equations will be derived and evaluated later as eqs.(2-41)' and (2-42)',

$$\mathcal{Y}_n(N) = Y_{on} \coth(N\xi_{nm}) \quad (2-1)$$

$$\mathcal{Y}_c(N) = Y_{oc} \tanh(N\xi_{mc}) \quad (2-2)$$

where N is the number of cell and ξ_{mp} is the phase advance per cell and is expressed by eqs. (2-33). The formulae of the common mode depend on the terminal condition at the end of the magnet string. The formulae of the normal mode are the same for any type of magnet string. Equations (2-1) and (2-2) form the bases of the present analysis in the frequency and the time domain.

The equations above show at the output of the power supply that the existence of N parallel and series resonances. The series resonance is excited when the denominator of the hyperbolic tangent and hyperbolic cotangent

function takes the minimum value and the parallel resonance is excited when the numerator of these functions takes the minimum value. The amplitude of the admittance at the resonant frequency depends upon a magnitude of the resistance in parallel to the inductance. Parallel resistance is not infinite even when the bridge resistor is not connected due to an AC loss of the magnet. Resonance of the lowest frequency appears as a parallel resonance for the normal mode admittance. The lowest resonant frequency of the common mode appears as the series resonance. In many synchrotrons, where the midpoint of the magnet string is floated, the common mode resonance is of more problem than the normal mode resonance. As they do not provide the common mode low pass filter, the amplitude of the common mode voltage ripple is larger than that of the normal mode voltage, and this resulted in a non-negligible amount of ripple current in the load.

From a comparison with a measurement of the admittance of the actual load, it is better to introduce a resistor of several $k\Omega$ in parallel with the excitation coil in the model to have good experimental fitting between the model and the observation. This resistance is interpreted as an equivalent AC loss of the magnet. With this parallel resistor, the amplitude of the resonance of higher frequency is more damped than that of lower frequency. The magnitude of the capacitance to the ground is about 1.8 nF which is estimated from the comparison of a small signal measurement. The stray capacitance and the bridge resistor were also conceived by Snowdon for the Fermilab main ring magnet but not as the ladder circuit[22]. In the present model, the magnitude of the inductance, resistance, capacitance are treated as constant for simplicity. In reality, they may vary with frequency or current level. This approximation causes the deviation between the observation and the estimated value but essential property is still held to be true.

In Figure 3, the calculated admittance of the Focussing Quadrupole of the HIMAC is shown with no external bridge resistor. Throughout this article, the calculation is performed using Mathcad[21]. Figure 4 shows the calculated admittance of the Quadrupole with the external bridge resistor of 20 Ω . As the frequency increases, the resonance is gradually damped and approaches to a constant value, which is a characteristic impedance of the ladder circuit as shown in Figure 3. In the simplest approximation of the single lumped element of the inductance and the capacitance, the normal mode admittance of the magnet load decreases in proportion to the increasing frequency. In

this case, the common mode admittance increases infinitely with increasing frequency. The measured admittance in a small signal excitation using four channel FFT analyzer and a power amplifier and the calculation based on this model roughly agrees[2]. These observed admittance are used to calculate the current in the load from applied voltage to the load for frequencies higher than 1200 Hz.

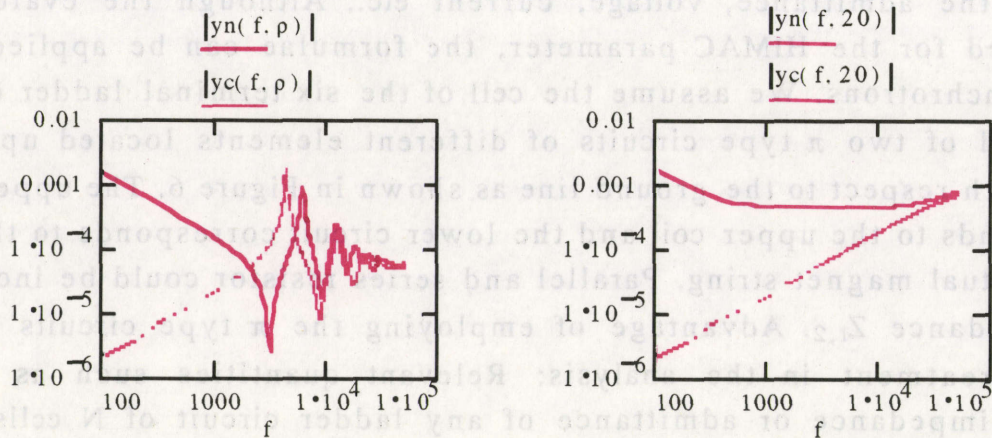


FIGURE 3&4. The normal and common mode admittance(calculated) of the HIMAC Quadrupole magnet without the bridge resistor(left) and with bridge resistor(right). $\rho = 6 \text{ k}\Omega$ (equivalent resistance, Figure3). The stray capacitance of 1.8 nF. The resistance of the bridge resistor is $\rho = 20 \text{ }\Omega$ (Figure4).

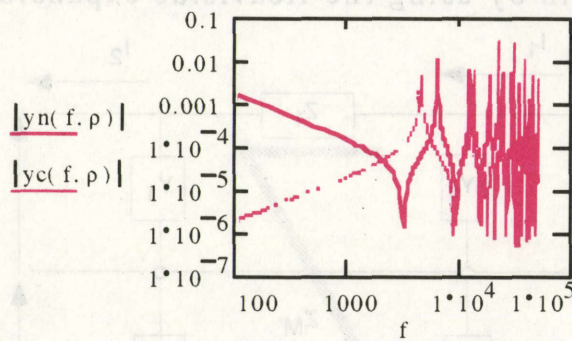


FIGURE 5. The normal and common mode admittance (calculated) of the HIMAC Quadrupole magnet without the bridge resistor. $\rho = 6 \text{ M}\Omega$ is assumed to emphasize the resonance.

With an installment of a bridge resistor, $\rho = 20 \text{ }\Omega$ for the Quadrupole and $100 \text{ }\Omega$ for the dipole, in parallel to the coil, the resonance is completely damped as shown in Figure 4. Figure 5 shows the calculated admittance when the external bridge resistor is high to emphasize the resonance. Three figures above shows a marked contrast of the effect of the bridge resistor.

The magnitude of the bridge resistor chosen is less than that required to simply damp the resonance. This is because the bridge resistor is used to bypass the logical ripple in addition to damping the resonance of a thyristor spike.

In the following, we will derive the equations above to evaluate variables such as the admittance, voltage, current etc.. Although the evaluation is performed for the HIMAC parameter, the formulae can be applied to any other synchrotrons. We assume the cell of the six terminal ladder circuit is composed of two π type circuits of different elements located upper and lower with respect to the ground line as shown in Figure 6. The upper circuit corresponds to the upper coil and the lower circuit corresponds to the lower coil in actual magnet string. Parallel and series resistor could be included in the impedance $Z_{1,2}$. Advantage of employing the π type circuits is in its simple treatment in the analysis: Relevant quantities such as voltage, current, impedance or admittance of any ladder circuit of N cells can be expressed by a combination of complex sinusoidal function or hyperbolic sinusoidal function. The parameters of magnet string of any N cells are expressed by simple analytic expressions in a closed form. This modal expression also enables us to construct analytic expressions of a transient response in time domain by using the Heaviside expansion theorem.

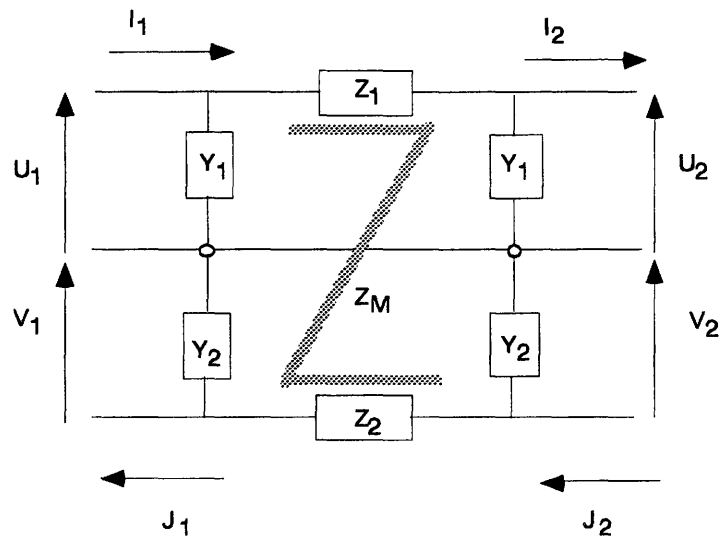


FIGURE 6. Model circuit of the cell of the six terminal circuit in a presence of upper and lower asymmetry. The impedance of the upper coil Z_1 and the lower coil Z_2 are coupled through the iron yoke of the same magnet to a separate connection.

Ladder circuit consists of a repeated circuit of cascaded cells of lumped elements. Cell consists of self inductance L_1 and L_2 and mutual inductance M_{12} and M_{21} , and resistance r_1 and r_2 of the excitation coil and capacitance C_1 and C_2 assumed to be connected in parallel between the iron core and the coil. Here $Z_1=sL_1+r_1, Z_2=sL_2+r_2$ and $Y_1=sC_1, Y_2=sC_2$. Additional resistor ρ parallel to the coil is also incorporated in the cell. This resistor ρ represents the bridge resistor. In absence of the bridge resistor, ρ is still necessary in the model to take into account an equivalent loss of the magnet which is determined experimentally.

Capacitance to the ground yoke can be treated as distributed element rather than concentrated element. It may not be uniformly distributed along the direction of the multi-layered pancake coil. Furthermore, the inductance and the resistance are frequency dependent. To take into account all these details may be possible at a cost of complexity. The choice of a model depends what should one clarify by analyzing the model. If only the DC characteristic or the low frequency illogical ripple is required to be evaluated, the model of the concentrated circuit without the capacitance is enough. Snowdon conceived this capacitor once but neglected in his calculation as he is not interested in high frequency ripple or spike[22]. In reality, the thyristor spike with frequency beyond a few kHz modulated by lower illogical ripple is observed. The model that can allow for treating the ignition spikes and resonances in the power supply system is required.

Transmission line model[9,10,11,12,13,14,15] is capable of treating the circuit to very high frequency. On the other hand, it is inconvenient to mix a lumped element of the bridge resistor with a distributed circuit. We chose the π -type cell model of the lumped elements of constant magnitude, which is independent on the frequency and the level of the excitation to avoid unnecessary complexity of the analysis without a loss of essential elements.

General Formulation

We consider a model circuit of the cell of the six terminal circuit in case of upper and lower asymmetry as shown in Figure 6. The impedance of the upper coil Z_1 and the lower coil Z_2 are coupled through the iron yoke of the

same magnet. Let us designate the relevant parameter of the voltage and the current above the earth line as U and I and below as V and J with a suffix of the input and output designated as 1 and 2. Applying the Kirchhoff law, we have following equations to a first order approximation,

$$U_1 = Z_1(I_1 - U_1 Y_1) + Z_{M12}(J_1 - V_1 Y_2) + U_2 \quad (2-3)$$

$$V_1 = Z_2(J_1 - V_1 Y_2) + Z_{M21}(I_1 - U_1 Y_1) + V_2 \quad (2-4)$$

$$I_2 = I_1 - U_1 Y_1 + U_2 Y_1 \quad (2-5)$$

$$J_2 = J_1 - V_1 Y_2 - V_2 Y_2. \quad (2-6)$$

One then can write down the equations in a following form,

$$\begin{bmatrix} U_1 \\ I_1 \\ V_1 \\ J_1 \end{bmatrix} = \begin{bmatrix} 1+Z_1 Y_1 & Z_1 & Z_{M2} Y_2 & Z_{M2} \\ Y_1(2+Z_1 Y_1) & 1+Z_1 Y_1 & Z_{M1} Y_1 Y_2 & Z_{M2} Y_1 \\ Z_{M1} Y_1 & Z_{M1} & 1+Z_2 Y_2 & Z_2 \\ Z_{M1} Y_1 Y_2 & Z_{M1} Y_2 & Y_2(2+Z_2 Y_2) & 1+Z_2 Y_2 \end{bmatrix} \begin{bmatrix} U_2 \\ I_2 \\ V_2 \\ J_2 \end{bmatrix} \quad (2-7)$$

with $Z_M = Z_{M1} = sM_{12} = Z_{M2} = sM_{21}$ and "s" is a Laplace differential operator. Non-zero mutual inductance Z_M is due to the magnetic coupling through the yoke. This is a characteristic feature of a separate connection of the upper and the lower coil of the HIMAC magnet. Apparently the voltage and the current of the π circuit of the upper coil and the lower coils are coupled by the iron yoke in separate connected cell. The analysis needs the manipulation of four by four matrix in this form. By intuition, eq.(2-7) is tedious to solve as one needs to solve by four by four matrix. This equation can be transformed into the following expression of the normal mode and the common mode equations of the voltage and the current flowing in the P and N lines and the ground lines. This transformation can be devised logically from the eigenvalue method as shown in later section.

$$\begin{bmatrix} U_1+V_1 \\ I_1+J_1 \\ U_1-V_1 \\ I_1-J_1 \end{bmatrix} = T \cdot \begin{bmatrix} U_2+V_2 \\ I_2+J_2 \\ U_2-V_2 \\ I_2-J_2 \end{bmatrix} \quad (2-8)$$

where the transfer matrix T is written as,

$$T = \begin{bmatrix} \frac{1}{2} \begin{bmatrix} 1+ \\ [Z_1+Z_M]Y_1+ \\ [Z_2+Z_M]Y_2 \end{bmatrix} & \frac{1}{2} [Z_1+Z_2+2Z_M] & \frac{1}{2} \begin{bmatrix} [Z_1+Z_M]Y_1- \\ [Z_2+Z_M]Y_2 \end{bmatrix} & \frac{1}{2} [Z_1-Z_2] \\ \frac{1}{2} \begin{bmatrix} Y_1(2+Z_1Y_1 \\ +Z_M Y_2)+ \\ Y_2(2+Z_2Y_2 \\ +Z_M Y_1) \end{bmatrix} & \frac{1}{2} \begin{bmatrix} 1+ \\ [Z_1+Z_M]Y_1+ \\ [Z_2+Z_M]Y_2 \end{bmatrix} & \frac{1}{2} \begin{bmatrix} Y_1[2+Z_1Y_1+Z_M Y_2]- \\ Y_2[2+Z_2Y_2+Z_M Y_1] \end{bmatrix} & \frac{1}{2} \begin{bmatrix} [Z_1-Z_M]Y_1- \\ [Z_2-Z_M]Y_2 \end{bmatrix} \\ \frac{1}{2} \begin{bmatrix} [Z_1-Z_M]Y_1- \\ [Z_2-Z_M]Y_2 \end{bmatrix} & \frac{1}{2} [Z_1-Z_2] & \frac{1}{2} \begin{bmatrix} 1+ \\ [Z_1-Z_M]Y_1+ \\ [Z_2-Z_M]Y_2 \end{bmatrix} & \frac{1}{2} [Z_1+Z_2-2Z_M] \\ \frac{1}{2} \begin{bmatrix} Y_1[2+Z_1Y_1-Z_M Y_2]- \\ Y_2[2+Z_2Y_2-Z_M Y_1] \end{bmatrix} & \frac{1}{2} \begin{bmatrix} [Z_1+Z_M]Y_1- \\ [Z_2+Z_M]Y_2 \end{bmatrix} & \frac{1}{2} \begin{bmatrix} Y_1[2+Z_1Y_1-Z_M Y_2]+ \\ Y_2[2+Z_2Y_2-Z_M Y_1] \end{bmatrix} & \frac{1}{2} \begin{bmatrix} 1+ \\ [Z_1-Z_M]Y_1+ \\ [Z_2-Z_M]Y_2 \end{bmatrix} \end{bmatrix} \quad (2-9)$$

Due to a hardware imperfection, difference in magnitude of the inductance and the capacitance between the upper and the lower coils is inevitable and is expressed by ΔL and ΔC as depicted in Figure 7.

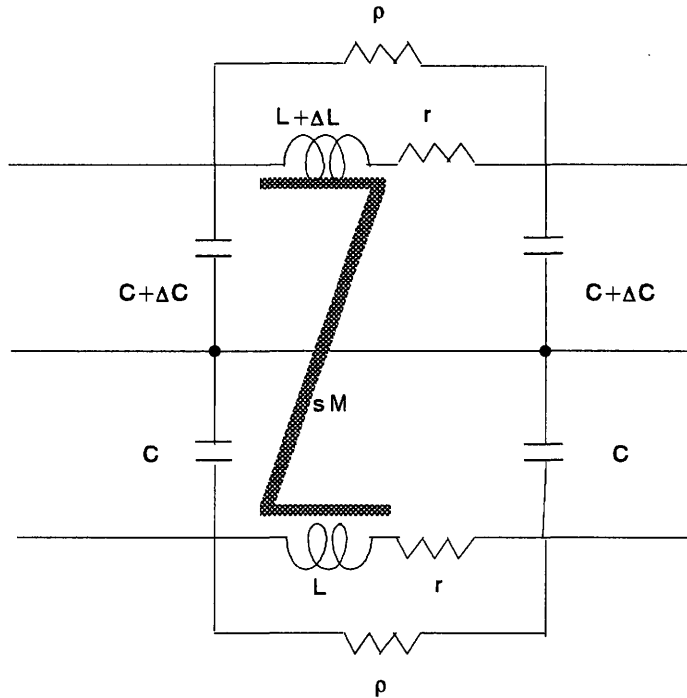


FIGURE 6. Model circuit of the asymmetric six terminal circuit.

The inductance and the capacitance are assumed to be slightly

different between the upper and the lower coils by ΔL and ΔC .

Then eq.(2-9) is reduced to eq. (2-10).

$$T = \begin{bmatrix} 1 + sC[s(L+M)+r] & s(L+M)+r & \frac{1}{2} \left[\begin{array}{l} s^2\Delta LC + \\ s[s(L+M)+r]\Delta C \end{array} \right] & \frac{1}{2} s\Delta L \\ sC \left[\begin{array}{l} 2 + \\ [s(L+M)+r]sC \end{array} \right] & 1 + [s(L+M)+r]sC & \frac{sC}{2} \left[\begin{array}{l} \frac{\Delta C}{C} [1+s^2LC] \\ +s^2\Delta LC \end{array} \right] & \frac{s^2}{2} \left[\begin{array}{l} \Delta LC + \\ (L-M)\Delta C \end{array} \right] \\ \frac{s^2}{2} \left[\begin{array}{l} \Delta LC + \\ (L-M)\Delta C \end{array} \right] & \frac{1}{2} s\Delta L & 1 + sC[s(L-M)+r] & s(L-M)+r \\ \frac{sC}{2} \left[\begin{array}{l} \frac{\Delta C}{C} [1+s^2LC] \\ +s^2\Delta LC \end{array} \right] & \frac{1}{2} \left[\begin{array}{l} s^2\Delta LC + \\ s[s(L+M)+r]\Delta C \end{array} \right] & sC \left[\begin{array}{l} 2 + \\ [s(L-M)+r]sC \end{array} \right] & 1 + [s(L-M)+r]sC \end{bmatrix} \quad (2-10)$$

where $Z_1=sL+r$, $Y_1=sC$, $Y_1-Y_2=s\Delta C$ and $Z_1-Z_2=s\Delta L$ are assumed.

Every component in the transfer matrix T is non-zero and has finite value. The circuit expressed by four by four matrixes is known in a microstrip circuit of two signal lines and one earth line, and has been extensively studied in the field of the microwave theory where the two modes are called "even mode" and "odd mode" [19]. The pair of the voltage and current of (U,I) and (V,J) lead to two modes of the sum and the difference. The non-zero component of the matrix means that the two modes are effected each other. From the eqs.(2-10), when $\Delta L=\Delta C=0$, which is the case of a symmetry, one can easily show that the normal mode equations and the common mode equations are independent each other. Even in an absence of the symmetry, there is a general method to decouple the mode known as "eigenvalue problem". In order to extend the mode analysis of symmetry into an asymmetric configuration, how to decouple the mode is shown in the following

General Treatment of Mode Separation

Let us consider an asymmetric six terminal circuit as shown in Figure 7. For convenience, we use the transmission line equation. The transmission

line circuit is treated by taking L , C and r to be per unit length of the ladder circuit whereas in the ladder circuit they are treated as per unit magnet.

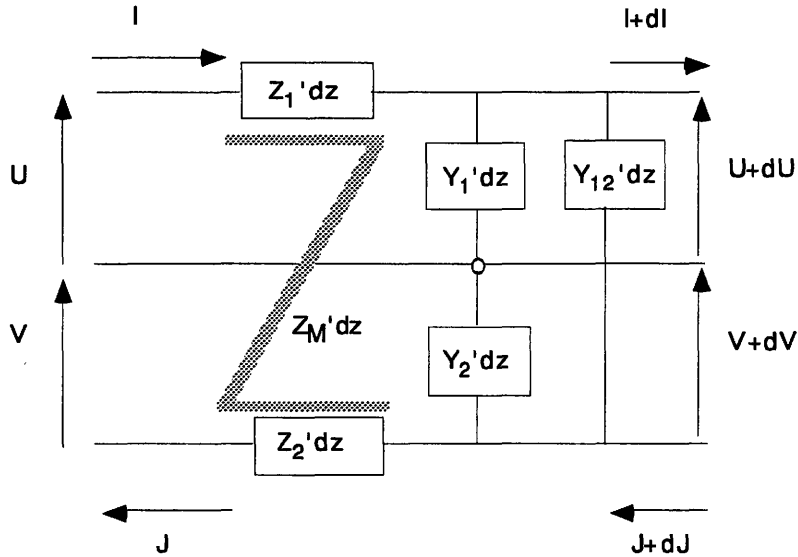


FIGURE 7. Equivalent circuit of the six terminal transmission line circuit per unit length. Prime denotes quantities per unit length.

(i) **Asymmetric Transfer Matrix**

Applying the Kirchhoff law in the circuit of Figure 8, we have following equations,

$$U = Z_1' Idz + Z_M' Jdz + U + dU \tag{2-11}$$

$$V = Z_2' Jdz + Z_M' Idz + V + dV \tag{2-12}$$

$$I = \{(U + dU)Y_1' + (U + V + dU + dV)Y_{12}'\} dz + I + dI \tag{2-13}$$

$$J = \{(V + dV)Y_1' + (U + V + dU + dV)Y_{12}'\} dz + J + dJ \tag{2-14}$$

To the first order approximation, we have the following coupled transmission equations for voltage of U and V ,

$$\frac{d^2 U}{d^2 z} = AU + BV \tag{2-15}$$

$$\frac{d^2 V}{d^2 z} = CU + DV \tag{2-16}$$

where A , B , C and D are assumed to be uniform along the coordinate z . They

are expressed by the following equations,

$$A = Z_1' Y_1' + 2Y_{12}'(Z_1' + Z_M') \quad (2-17)$$

$$B = Z_M' Y_1' + 2Y_{12}'(Z_1' + Z_M') \quad (2-18)$$

$$C = Z_M' Y_1' + 2(Z_2' + Y_M')Y_{12}' \quad (2-19)$$

$$D = Z_2' Y_2' + 2(Z_2' + Y_M')Y_{12}' \quad (2-20)$$

where again the prime denotes the impedance and the admittance per unit length. These equations are valid for the transmission line model and for the ladder circuit model; "z" is regarded as a coordinate along a propagation direction of the voltage wave for the former case and a discrete coordinate for the ladder circuit. Similar equation holds for the current I and J. Two set of equations show a presence of two modes of voltage and current in the magnet string. This formulation could be extended to N mode equations of a system of (N-1) signal lines and a single ground line. As is shown by the equations, voltage U and V are coupled. These coupled voltage propagates down the magnets. It is tedious to solve two simultaneous second order differential equations. There is an established method to solve this problem known as an eigenvalue problem. In eigenvalue problem, mode-decoupling is done by finding a proper transformation matrix. What one need is to transform a matrix of,

$$M = \begin{bmatrix} A & B \\ C & D \end{bmatrix} \quad (2-21)$$

to a matrix M' designated as

$$M' = \begin{bmatrix} a & 0 \\ 0 & d \end{bmatrix} \quad (2-22)$$

i.e., the diagonalization of the transfer matrix M is required.

After some manipulations, one can find, multiplication of a following matrix P from the right and P⁻¹ from the left to M:

$$M' = P^{-1} M P \quad (2-23)$$

with

$$P = \begin{bmatrix} 1 & \frac{q}{C} \\ \frac{q}{B} & -1 \end{bmatrix} \quad (2-24)$$

where q is expressed as,

$$q = \frac{1}{2} (A - D \pm \sqrt{(A - D)^2 + 4BC}) . \quad (2-25) \quad \text{The}$$

mode separation is possible by the transformation given above. This transformation enables us to find the analytical expression in a closed form in case of an asymmetric configuration. In the HIMAC, the magnitude and the location of every possible element are set to be the same as possible as we can with respect to the earth line defined as "symmetry". In this case, considerable simplification is possible as shown in the following.

(ii) Symmetric Transfer Matrix

In a symmetric case, where Z_{12} and Z_{21} are equal, one obtains for M' ,

$$M' = \begin{bmatrix} 1 & 1 \\ 1 & -1 \end{bmatrix} \quad (2-26)$$

Equation (2-26) shows two modes of coupled voltage is reduced to the decoupled sum and difference of the voltage. This is defined as the normal and common mode. In this case $\Delta L = \Delta C = 0$. Then, eq.(2-9) is reduced to,

$$\begin{bmatrix} U_1 + V_1 \\ I_1 + J_1 \\ U_1 - V_1 \\ I_1 - J_1 \end{bmatrix} = \begin{bmatrix} 1 + Z_{mn} Y_{mn} & Z_{mn} & 0 & 0 \\ Y_{mn}(2 + Z_{mn} Y_{mn}) & 1 + Z_{mn} Y_{mn} & 0 & 0 \\ 0 & 0 & 1 + Z_{mc} Y_{mc} & Z_{mc} \\ 0 & 0 & Y_{mc}(2 + Z_{mc} Y_{mc}) & 1 + Z_{mc} Y_{mc} \end{bmatrix} \begin{bmatrix} U_2 + V_2 \\ I_2 + J_2 \\ U_2 - V_2 \\ I_2 - J_2 \end{bmatrix} \quad (2-27)$$

where Z_{mn} , Z_{mc} , Y_{mn} , and Y_{mc} , mean the normal mode impedance, the common mode impedance, the normal mode admittance and the common mode admittance defined as,

$$Z_{mn} = \frac{1}{\frac{1}{sL_n} + \frac{1}{\rho}} = \frac{1}{\frac{1}{s(L+M)+r} + \frac{1}{\rho}} \quad (2-28)$$

$$Z_{mc} = \frac{1}{\frac{1}{sL_c} + \frac{1}{\rho}} = \frac{1}{\frac{1}{s(L-M)+r} + \frac{1}{\rho}} \quad (2-29)$$

$$Y_{mn} = sC_n = sC \quad (2-30)$$

$$Y_{mc} = sC_c = sC \quad (2-31)$$

where ρ represents the bridge resistor or the equivalent resistance due to the ac loss of the magnet. In the HIMAC, the common mode inductance of the Bending magnet is less than 1% of the normal mode inductance. The common mode inductance of the Quadrupole magnet is about half of the normal mode

inductance.

Due to the transformation, the original coupled mode of the variables of $(U, I), (V, J)$ is reduced to the normal and common mode of $(U+V, I+J), (U-V, I-J)$. The unit cell thus is expressed in a unified fashion as shown in Figure 9, where u_p stands for $U \pm V$, and i_p stands for $I \pm J$, with $p=n$ for the normal mode and $p=c$ for the common mode.

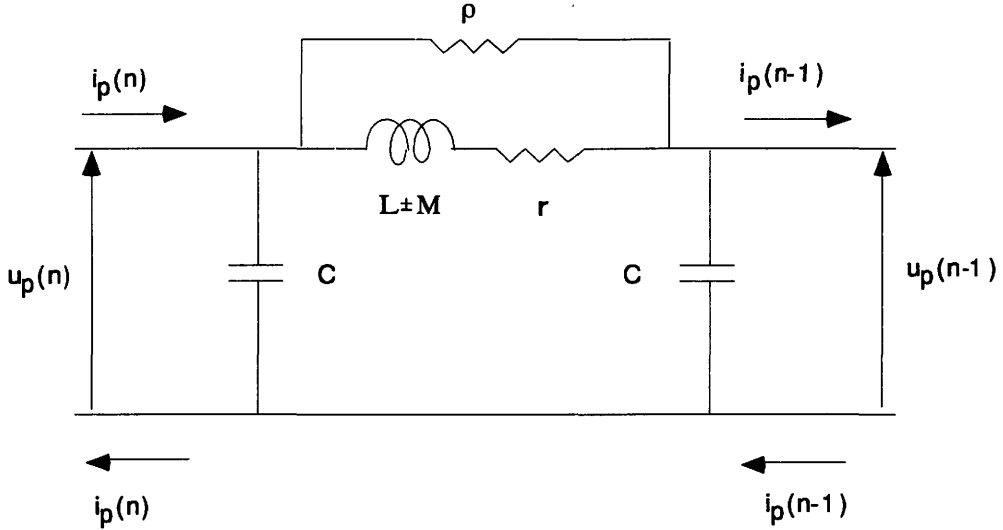


FIGURE 9. Four terminal π type equivalent circuit reduced from the six terminal circuit. For normal mode($p=n$) inductance and capacitance are $L+M$ and C . For common mode($p=c$), they are $L-M$ and C .

One can write down the decoupled equations of each mode. One considers the four terminal ladder circuits of N cascaded ladder circuit of π -type. The number of the cells is counted from the end of the magnet string, namely the N -th magnet is located at the input of the magnet string. It is assumed that the end of the Positive and Negative line is terminated by the impedance Z_E to the earth line in order not to lose a generality. Expressing the voltage and the current as $u_p(0)$ and $i_p(0)$ at the end of the furthest magnet and input as $u_p(N)$ and $i_p(N)$ we can define following equation,

$$\begin{bmatrix} u_p(N) \\ i_p(N) \end{bmatrix} = \begin{bmatrix} 1 + Z_{mp} Y_{mp} & Z_{mp} \\ Y_{mp} [2 + Z_{mp} Y_{mp}] & 1 + Z_{mp} Y_{mp} \end{bmatrix}^N \begin{bmatrix} u_p(0) \\ i_p(0) \end{bmatrix}$$

$$= \begin{bmatrix} \cosh(N\zeta_{mp}) & Z_{0p} \sinh(N\zeta_{mp}) \\ \frac{\sinh(N\zeta_{mp})}{Z_{0p}} & \cosh(N\zeta_{mp}) \end{bmatrix} \begin{bmatrix} u_p(0) \\ i_p(0) \end{bmatrix} \quad (2-32)$$

where ζ_{mp} and Z_{0p} are the transfer constant and the characteristic impedance defined as,

$$\cosh \zeta_{mp} \equiv 1 + Z_{mp} Y_{mp} \quad (2-33)$$

$$Y_{0p} \equiv \frac{1}{Z_{0p}} = \frac{\sinh \zeta_{mp}}{Z_{mp}} = \frac{Y_{mp} \sinh \zeta_{mp}}{\cosh \zeta_{mp} - 1} \quad (2-34)$$

$$= \left[\frac{Z_{mp}}{[2 + Z_{mp} Y_{mp}] Y_{mp}} \right]^{-\frac{1}{2}} \quad (2-35)$$

where Z_{mp} , Y_{mp} are the impedance and the admittance of the cell of the normal mode ($p=n$) and the common mode ($p=c$). The characteristic impedance of the admittance of the ladder circuit slightly differs from those of the transmission line circuit by factor $Z_{mp} Y_{mp}$. This factor is small at a frequency range below the resonance frequency. In the case of the normal and the common mode, the normal and the common mode impedance are expressed with suffixes with n and c and defined by (U, V) and (I, J) are,

$$Z_{mn} = \frac{U + V}{I + J} \quad (2-36)$$

$$Y_{mn} = \frac{I + J}{U + V} \quad (2-36)'$$

$$Z_{mc} = \frac{U - V}{I - J} \quad (2-37)$$

$$Y_{mc} = \frac{I - J}{U - V} \quad (2-37)'$$

As is shown by the definition of the common mode admittance, the common mode inductance is very small, when the upper and the lower coils are separately connected. The magnitude is the order of the imperfection of the inductance of the upper coil and the lower coil.

Terminating the end of the magnet string with Z_{Ep} ,

$$u_p(0) = Z_{Ep} i_p(0) \quad (2-38)$$

Voltage of the n-th magnet is,

$$u_p(n) = u_p(N) \frac{Z_{Ep} \cosh(n\zeta_{mp}) + Z_{0p} \sinh(n\zeta_{mp})}{Z_{Ep} \cosh(N\zeta_{mp}) + Z_{0p} \sinh(N\zeta_{mp})} \quad (2-39)$$

The input impedance \mathcal{Z}_p of the magnet string is thus,

$$\mathcal{Z}_p(N) = \frac{u_p(N)}{i_p(N)} = Z_{0p} \frac{Z_{Ep} \cosh(N\zeta_{mp}) + Z_{0p} \sinh(N\zeta_{mp})}{Z_{Ep} \sinh(N\zeta_{mp}) + Z_{0p} \cosh(N\zeta_{mp})} \quad (2-40)$$

These equations above are valid for the normal and the common mode. With the termination condition of $Z_{Ep}=0$ at the end, the voltage is zero, and the normal mode impedance \mathcal{Z}_n and the admittance \mathcal{Y}_n are written as,

$$\mathcal{Z}_n = \mathcal{Z}_n(N) = Z_{0n} \tanh(N\zeta_{mn}) \quad (2-41)$$

$$\mathcal{Y}_n = \mathcal{Y}_n(N) = Y_{0n} \coth(N\zeta_{mn}) \quad (2-41)'$$

Eq.(2-1) is derived from the eq.(2-41). We have the open-ended condition, $Z_{Ec}=\infty$, the current is zero, at the end for the common mode in the HIMAC. Thus, the common mode input impedance \mathcal{Z}_c and the admittance \mathcal{Y}_c of the magnet string is,

$$\mathcal{Z}_c = \mathcal{Z}_c(N) = Z_{0c} \coth(N\zeta_{mc}) \quad (2-42)$$

$$\mathcal{Y}_c = \mathcal{Y}_c(N) = Y_{0c} \tanh(N\zeta_{mc}) \quad (2-42)'$$

Eqs.(2-1) and (2-2) or Eqs.(2-41)' and (2-42)' are the most basic equations in this analysis. When it is seen from the power supply side, any magnet string with repeated nature can be described by these simple equations.

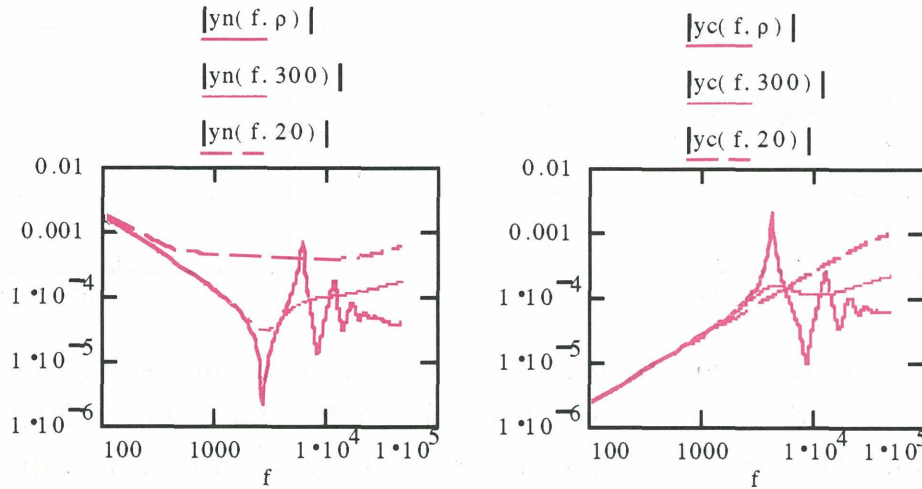


FIGURE 10 & 11. Normal mode and common mode admittance of the HIMAC Quadrupole magnet string for the bridge resistor of $\rho=6 \text{ k}\Omega$, 300Ω and 20Ω .

As a summary of the voltage and the current of the n -th cell for the normal and the common mode, one can write,

$$u_n(n) = u_n(N) \frac{\sinh(n\zeta_{mn})}{\sinh(N\zeta_{mn})} \quad (2-43)$$

$$i_n(n) = i_n(N) \frac{\cosh(n\zeta_{mn})}{\cosh(N\zeta_{mn})} = u_n(N) Y_{0n} \frac{\cosh(n\zeta_{mn})}{\sinh(N\zeta_{mn})} \quad (2-44)$$

$$u_c(n) = u_c(N) \frac{\cosh(n\zeta_{mc})}{\cosh(N\zeta_{mc})} \quad (2-45)$$

$$i_c(n) = u_c(N) \frac{\sinh(n\zeta_{mc})}{\sinh(N\zeta_{mc})} = u_c(N) Y_{0c} \frac{\sinh(n\zeta_{mc})}{\cosh(N\zeta_{mc})} \quad (2-46)$$

where the suffix n and c stand for the normal and common mode. Using the equations above, the voltage and the current are calculated and plotted in the following.

Frequency Characteristics of Voltage

Frequency characteristic of the voltages of the typical cell of the normal and the common mode are shown in Figure 12 and 13 without and with the bridge resistor ($\rho=20\Omega$). The resonance is shown to be completely removed by the bridge resistor.

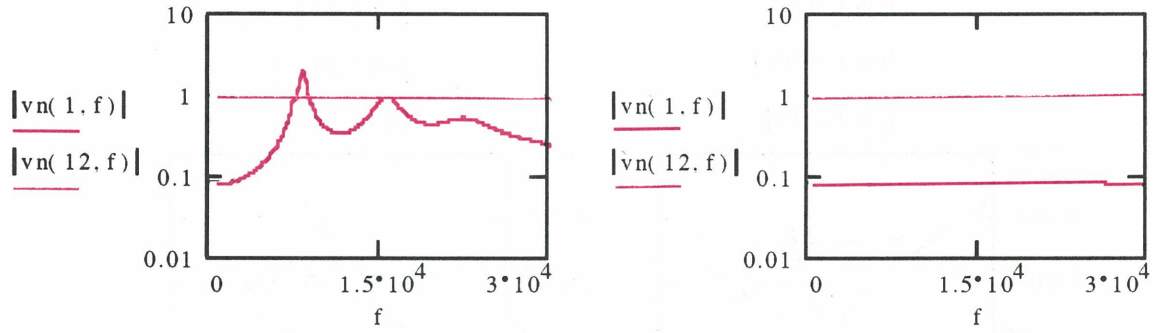


FIGURE 12. Normal mode frequency characteristic of the voltages of the typical cell($n=1$ and 12) of without($\rho=6$ k Ω , left) and with($\rho=20\Omega$, right) the bridge resistor. The $vn(n,f)$ stands for the voltage of n -th cell with the frequency of f .

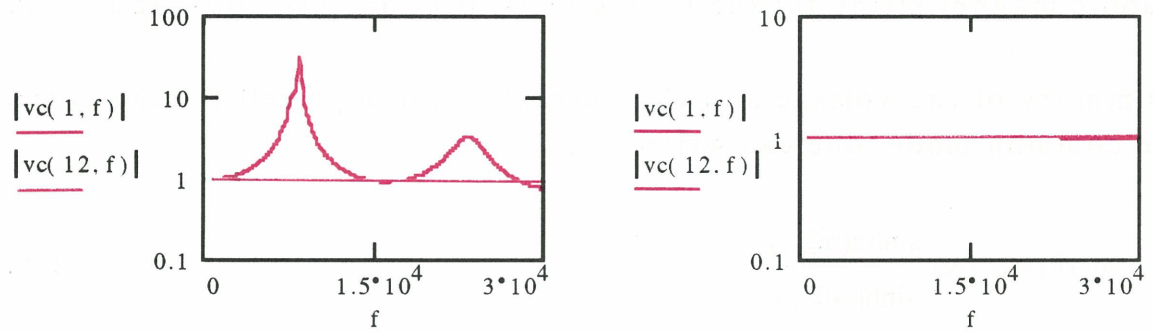


FIGURE 13. Common mode frequency characteristic of the voltages of the typical cell($n=1$ and 12) of without($\rho=6$ k Ω , left) and with($\rho=20\Omega$, right) the bridge resistor. The $vc(n,f)$ stands for the voltage of n -th cell with the frequency of f .

The current flowing in the coil of the magnet $i_{mp}(n)$ of n -th cell for both mode is obtained by dividing the applied voltage of the magnet by the impedance of the respective coil Z_{mp} of the magnet. The magnet coil current $i_{mp}(n)$ is written as,

$$i_{mp}(n) = \frac{u_p(N)}{Z_{mp}} \frac{[Z_{Ep} [\cosh(n\zeta_{mp}) - \cosh[(n-1)\zeta_{mp}]] + Z_{Op} [\sinh(n\zeta_{mp}) - \sinh[(n-1)\zeta_{mp}]]]}{[Z_{Ep} \cosh(N\zeta_{mp}) + Z_{Op} \sinh(N\zeta_{mp})]} \quad (2-47)$$

Eq.(2-47) is further simplified to,

$$i_{mp}(n) = 2 \frac{u_p(N)}{Z_{mp}} \frac{\left[Z_{Ep} \sinh \left[\left(n - \frac{1}{2} \right) \zeta_{mp} \right] + Z_{Op} \cosh \left(n - \frac{1}{2} \right) \zeta_{mp} \right] \sinh \left(\frac{1}{2} \zeta_{mp} \right)}{\left[Z_{Ep} \cosh(N \zeta_{mp}) + Z_{Op} \sinh(N \zeta_{mp}) \right]} \quad (2-48)$$

The normal mode and the common mode current in the coil of the magnet in the HIMAC are thus written as,

$$i_{mn}(n) = 2 \frac{u_n(N)}{Z_{mn}} \frac{\cosh \left[\left(n - \frac{1}{2} \right) \zeta_{mn} \right] \sinh \left[\frac{1}{2} \zeta_{mn} \right]}{\sinh(N \zeta_{mn})} \quad (2-49)$$

$$i_{mc}(n) = 2 \frac{u_c(N)}{Z_{mc}} \frac{\sinh \left[\left(n - \frac{1}{2} \right) \zeta_{mc} \right] \sinh \left[\frac{1}{2} \zeta_{mc} \right]}{\cosh(N \zeta_{mc})} \quad (2-50)$$

where $Z_{En} = 0$ for the normal mode and $Z_{Ec} = \infty$ for the common mode.

The equations above show the series and parallel resonance for the voltage and magnet current of the normal and common mode. The resonant frequencies for them are derived by the resonant condition;

$$1 + Z_{mn} Y_{mn} = \cosh \left(j \frac{k\pi}{N} \right) \quad (2-51)$$

$$1 + Z_{mc} Y_{mc} = \cosh \left(j \frac{k\pi}{2N} \right) \quad (2-52)$$

where the suffix n and c denote the normal and common and k is a integer from 0 to N-1. Equations (2-51) and (2-52) gives the second order equation in "s" (Laplace differential operator). One can find the resonance frequency, attenuation parameter, a dispersion relation from these equations as shown in the next section.

Cable Current and Coil Current

Magnitude of the ripple is often evaluated by the output cable current as in this article. This current is not directly measured but calculated from the voltage ripple and the admittance of the magnet string for the frequency greater than a few kHz. Below a few kHz, the admittance of the excitation

coil, which can be simply written as,

$$Y_{mp} \approx (sL_p + r)^{-1} + \rho^{-1} = [s(L \pm M) + r]^{-1} + \rho^{-1},$$

can be used. What should be evaluated is the magnet current. Magnitude and the phase of this current varies with a location in the magnet string. If the coil current is not greater than the cable current, one can use the cable current which is easier to evaluate. To see how the magnet current and the cable current differ we plotted it as a ratio of the cable current to a magnet current. They are shown from Figures 14 to 15 with and without bridge resistor for the case of Quadrupole. Without bridge resistor, the magnet current is resonantly enhanced at particular frequencies. In this case, the cable current is under-evaluated. With bridge resistor installed as in the HIMAC, however, the magnet current becomes smaller than cable current.

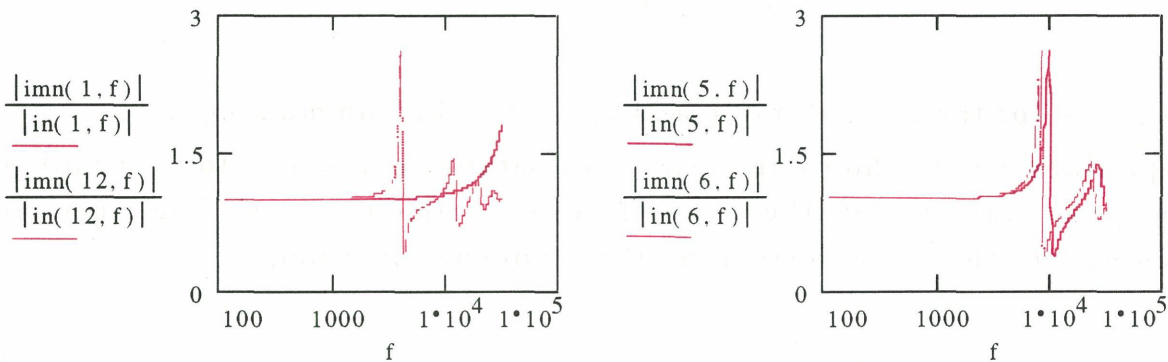


FIGURE14. Normal mode normalized magnet current without bridge resistor ($\rho=6 \text{ k}\Omega$, Quadrupole). $n=11$ and 12 for the left and $n=5$ and 6 for the right.

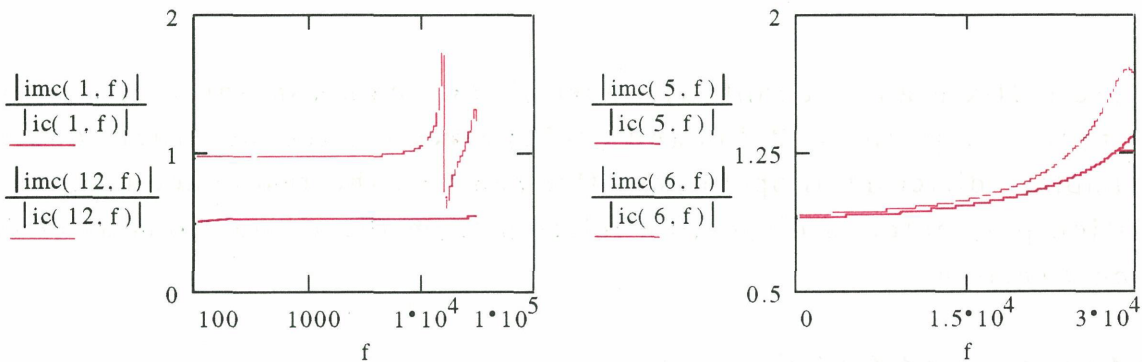


FIGURE15. Common mode normalized magnet current without bridge resistor ($\rho=6 \text{ k}\Omega$, Quadrupole). $n=1, 12, 5$ and 6 .

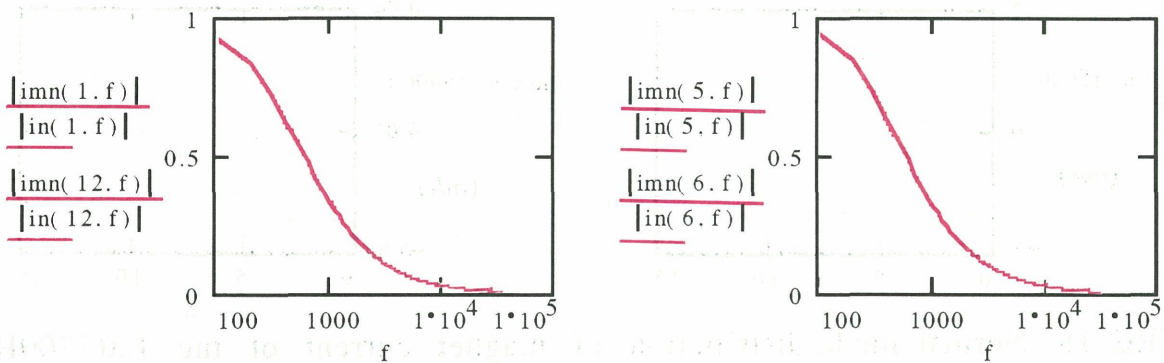


FIGURE 16. Normal mode normalized magnet current with bridge resistor ($\rho=20 \Omega$, Quadrupole). $n=1,12,5$ and 6 .

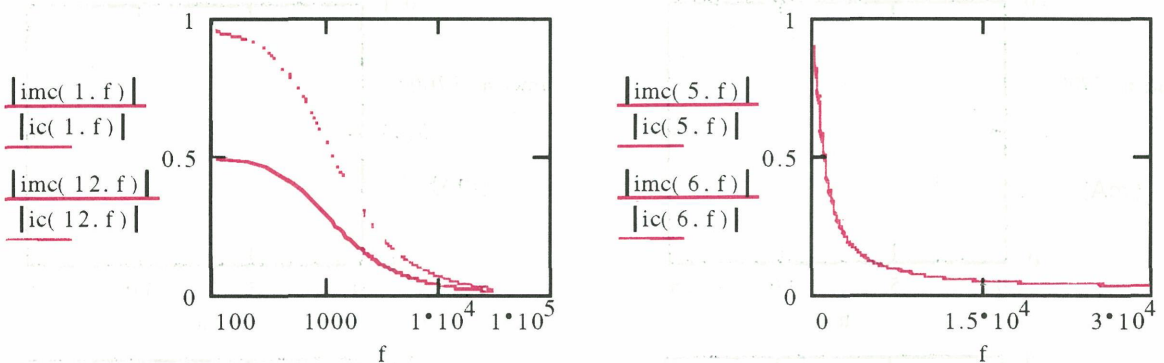
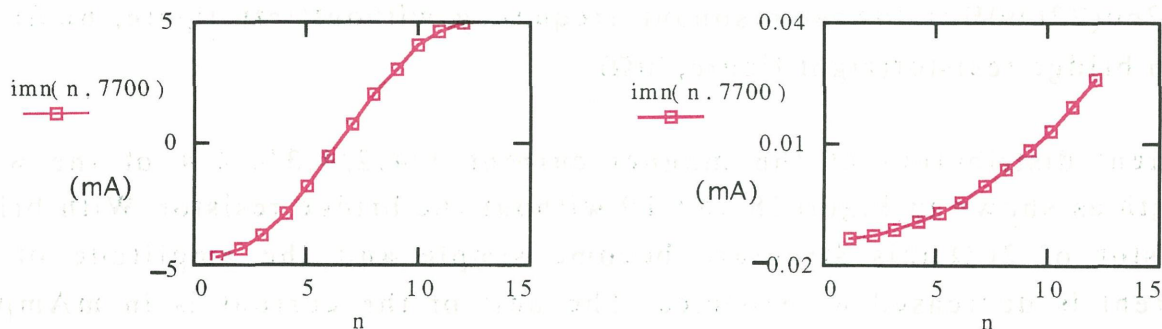


FIGURE 17. Common mode normalized magnet current of with bridge resistor ($\rho=20 \Omega$, Quadrupole). $n=1,12,5$ and 6 .

Spatial Distribution

The distribution of the magnet current varies along the magnet. Typical current patterns are shown below. The location of the power supply is at the right side of the figures.



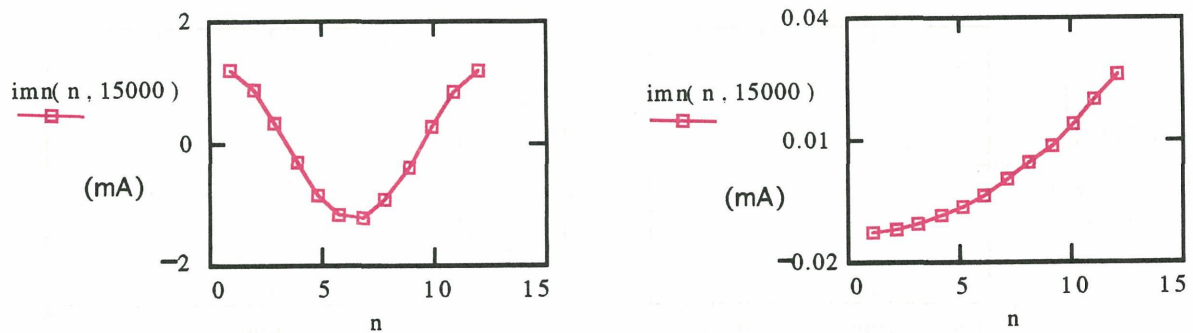


FIGURE 18. Normal mode distribution of magnet current of the 1st(7700Hz) and 2nd(15000Hz) lowest resonant frequency without(left figure, $6k\Omega$) and with bridge resistor(right figure, 20Ω)

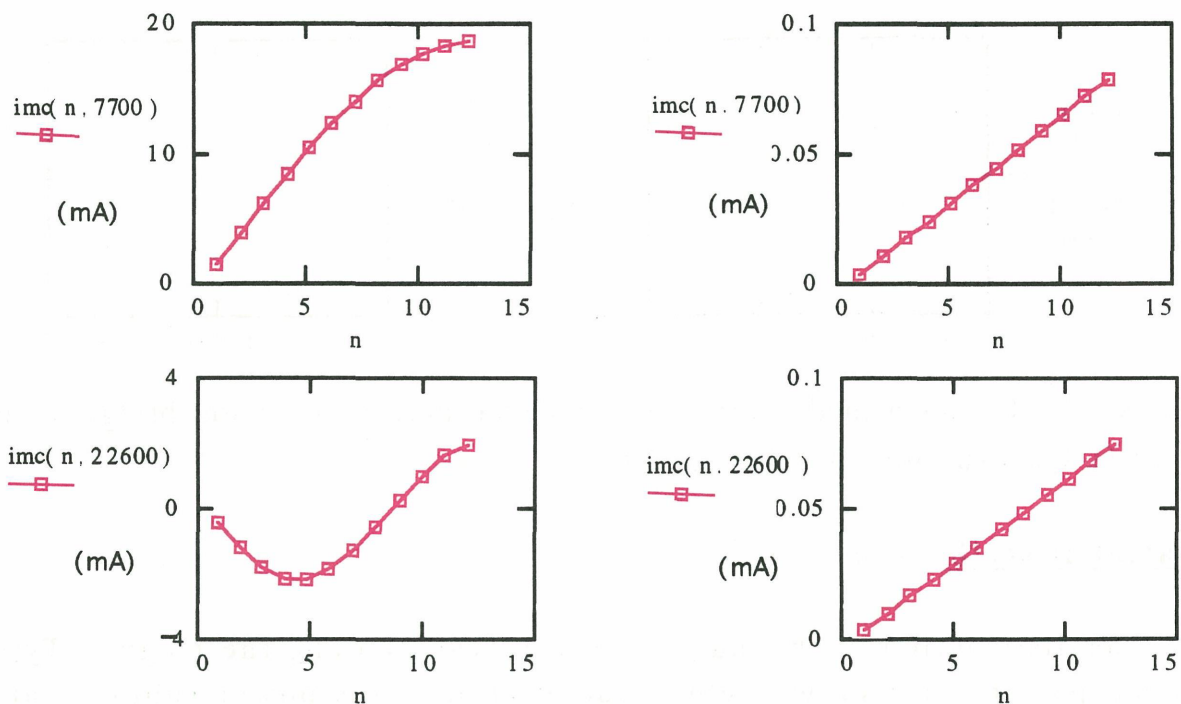


FIGURE 19. Common mode distribution of magnet current of the 1st(7700Hz) and 2nd(22600Hz) lowest resonant frequency without(left figure, $6k\Omega$) and with bridge resistor(right figure, 20Ω).

Current distribution of the magnet current $1/4, 2/4, 3/4, 4/4$ of the wave length as shown in Figure 18 and 19 without the bridge resistor. With bridge resistor of 20Ω this structure becomes simple and the amplitude of the current is decreased as expected. The unit of the current is in mA when the output voltage of the input of the magnet string is normalized to one volt.

Frequency Dependence of Magnet Coil Current

Frequency dependence of the magnet current depends on the location of the cell. Figure 20 and Figure 21 show typical examples. The lowest resonance frequency of the common mode is lower than that of the normal mode. Since the resonance of the lower frequency is stronger than that of the resonance of the higher frequency, one must avoid the resonance of the lower frequency.

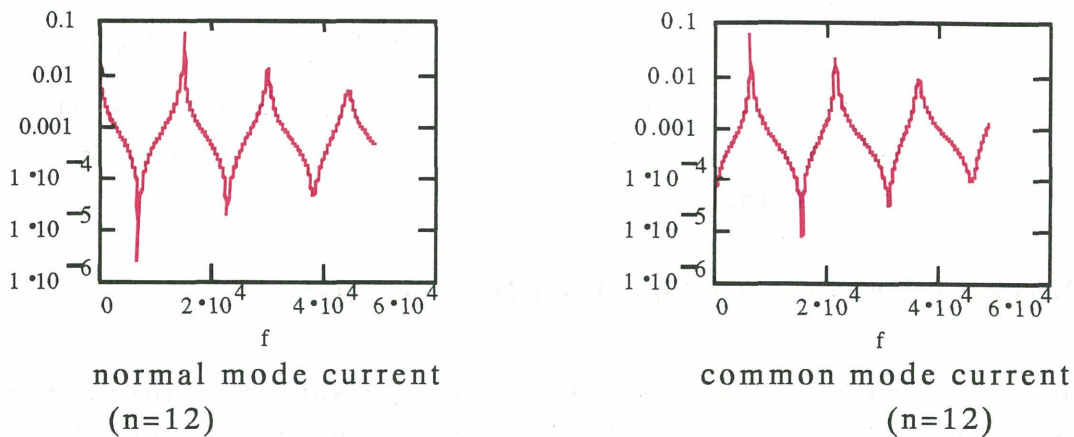


FIGURE 20. Frequency dependence of the magnet current of the n=12 magnet.

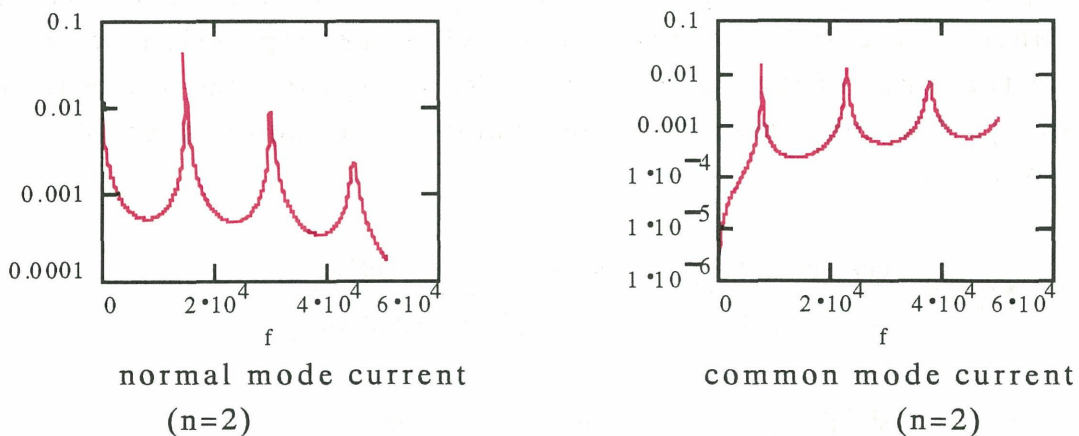


FIGURE 21. Frequency dependence of the magnet current of the n=2 magnet.

Impedance matching

To chose impedance matching is possible for the case of the common mode. The case of the impedance matching is interesting to evaluate, as in this case the frequency characteristic is rather flat and is independent on the frequency. The reflected wave in the time domain which may be often observed in several synchrotron magnet, is also expected to be considerably

suppressed. In the case of the impedance matching, where $Z_{Ep}=Z_{0p}$, we have, for the common mode cable current as,

$$\mathcal{Y}_e(N) = Y_{0c} \quad (2-53)$$

$$i_c(N) = Y_{0c} u_c(N) \quad (2-54)$$

$$i_{mc}(n) = \frac{[u_c(n) - u_c(n-1)]}{Z_{mc}} \\ = 2 \frac{u_c(n)}{Z_{mc}} e^{-N\zeta_{mc}} \left[\sinh \left[\left(n - \frac{1}{2} \right) \zeta_{mc} \right] + \cosh \left[\left(n - \frac{1}{2} \right) \zeta_{mc} \right] \right] \sinh \left(\frac{1}{2} \zeta_{mc} \right). \quad (2-55)$$

As shown, the resonance characteristic is disappeared for the case of impedance matching. Application of this case is interesting in other synchrotron magnet string.

III. Spike Analysis of the Ladder Circuit

Spike current is induced when the voltage source is abruptly changed. This is analyzed by the inverse Laplace transformation of the admittance or the impedance by multiplying the Laplace operator $1/s$. We use the admittance of the ladder circuit in deriving the expression of the current spike in the input of the magnet string. Recalling the admittance from eq.(2-41)' and (2-42)', and rewriting the characteristic admittance of the ladder circuit one has,

$$\mathcal{Y}_n = Y_{0n} \frac{\cosh(N\zeta_{mn})}{\sinh(N\zeta_{mn})} = Y_{mn} \frac{\sinh(\zeta_{mn})}{[\cosh(\zeta_{mn}) - 1]} \frac{\cosh(N\zeta_{mn})}{\sinh(N\zeta_{mn})} \quad (2-41)$$

$$\mathcal{Y}_e = Y_{0c} \frac{\sinh(N\zeta_{mc})}{\cosh(N\zeta_{mc})} = Y_{mc} \frac{\sinh(\zeta_{mc})}{[\cosh(\zeta_{mc}) - 1]} \frac{\sinh(N\zeta_{mc})}{\cosh(N\zeta_{mc})} \quad (2-42)'$$

for the normal mode and the common mode. The characteristic admittance \mathcal{Y}_p is written by the expression of the rational number. The denominator of the equation (2-1)' and (2-2)' can be decomposed. $\cosh(N\zeta_{mp})$ and $\sinh(N\zeta_{mp})$ can be expanded by $\cosh(\zeta_{mp})$ and can be expressed as a products of $\cosh(\zeta_{mp}) \pm \cos[k\pi/N]$. This process is equivalent to the process of the Heaviside theorem. For the even number of N that is the total number of cells, as in

the HIMAC Quadrupole string, we have[20],

$$\begin{aligned} \frac{\mathcal{Y}_s}{Y_{mm}} &= \frac{\sinh(\zeta_{mm})}{\left[\cosh(\zeta_{mm}) - 1\right]} \frac{\cosh(N\zeta_{mm})}{\sinh(N\zeta_{mm})} \\ &= \frac{2^{1-N}}{\cosh(\zeta_{mm}) \left[\cosh(\zeta_{mm}) - 1\right]} \frac{\cosh\left[N\zeta_{mm}\right]}{\prod_{k=1}^{\frac{N}{2}-1} \left[\cosh(\zeta_{mm}) + \cos\left[\frac{k\pi}{N}\right] \right] \left[\cosh(\zeta_{mm}) - \cos\left[\frac{k\pi}{N}\right] \right]} \end{aligned} \quad (3-1)$$

$$\begin{aligned} \frac{\mathcal{Y}_c}{Y_{mc}} &= \frac{\sinh(\zeta_{mc})}{\left[\cosh(\zeta_{mc}) - 1\right]} \frac{\sinh(N\zeta_{mc})}{\cosh(N\zeta_{mc})} \\ &= \frac{2^{1-N}}{\left[\cosh(\zeta_{mc}) - 1\right]} \frac{\sinh(\zeta_{mc}) \sinh(N\zeta_{mc})}{\prod_{k=0}^{\frac{N}{2}-1} \left[\cosh(\zeta_{mc}) + \cos\left[\frac{(2k+1)\pi}{2N}\right] \right] \left[\cosh(\zeta_{mc}) - \cos\left[\frac{(2k+1)\pi}{2N}\right] \right]} \end{aligned} \quad (3-2)$$

Similar equations can be obtained for odd number of N[20].

We have expanded the denominator in eqs.(3-1) and (3-2) by $\cosh(\zeta_{mp})$ so that the transformation to the Laplace operator is easy where the relation between them are written as,

$$1 + Z_{mp} Y_{mp} \equiv \cosh(\zeta_{mp}), \quad (3-3)$$

$$Z_{mp} Y_{mp} = 2 \sinh^2 \left[\frac{\zeta_{mp}}{2} \right]. \quad (3-4)$$

Keeping this relation in mind, one can further simplify the eqs.(3-1) and (3-2). Expansion of the eq.(3-1) by $\cosh[\zeta_{mp}/2]$ causes the range of summation to $k=1$ to $N-1$ from $k=1$ to $N/2-1$. Using the relation of $\cosh(x)=2\cosh^2(x)-1$, one can derive the following equations.

$$\frac{\mathcal{Y}_s}{Y_{mm}} = \frac{\prod_{k=0}^{N-1} \left[\cosh(\zeta_{mm}) - \cos\left[\frac{2k+1}{2N} \pi\right] \right]}{\prod_{k=0}^{N-1} \left[\cosh(\zeta_{mm}) - \cos\left[\frac{k}{N} \pi\right] \right]} \quad (3-5)$$

Similarly, for the common mode, one has,

$$\frac{Z_o}{Y_{mc}} = \frac{\prod_{k=1}^N \left[\cosh(\zeta_{mc}) - \cos \left[\frac{k}{N} \pi \right] \right]}{\prod_{k=0}^{N-1} \left[\cosh(\zeta_{mc}) - \cos \left[\frac{2k+1}{2N} \pi \right] \right]} \quad (3-6)$$

Putting $X_p = \cosh(\zeta_{mp})$, the numerator and the denominator are rational functions and are expressed by polynomials of X_p . The denominator and the numerator of the right hand side of the eqs.(3-5) and (3-6) have the order of N in X_p . Furthermore, the denominator and the numerator has no common factors. By dividing the numerator by the denominator, one can obtain the new numerator of the order of $(N-1)$ and the denominator of the order of N . One can apply the Heaviside expansion theorem. Thus the total admittance can be expressed as a sum of the partial fractional expression of X_p (Appendix).

Equations (3-5) and (3-6) are expressed as follows,

$$\frac{Z_o}{Y_{mn}} = 1 + \frac{1}{N} \sum_{k=0}^{N-1} \left[\frac{1 + \cos \left[\frac{k\pi}{N} \right]}{1 + Z_{mn} Y_{mn} - \cos \left[\frac{k\pi}{N} \right]} \right] = 1 + \frac{2}{N} \sum_{k=0}^{N-1} \left[\frac{\cos^2 \left[\frac{k\pi}{2N} \right]}{Z_{mn} Y_{mn} + \sin^2 \left[\frac{k\pi}{2N} \right]} \right], \quad (3-7)$$

$$\frac{Z_o}{Y_{mc}} = 1 + \frac{1}{N} \sum_{k=0}^{N-1} \left[\frac{1 + \cos \left[\frac{2k+1}{2N} \pi \right]}{1 + Z_{mc} Y_{mc} - \cos \left[\frac{2k+1}{2N} \pi \right]} \right] = 1 + \frac{2}{N} \sum_{k=0}^{N-1} \left[\frac{\cos^2 \left[\frac{2k+1}{4N} \pi \right]}{Z_{mc} Y_{mc} + \sin^2 \left[\frac{2k+1}{4N} \pi \right]} \right]. \quad (3-8)$$

Residues of above equations, which gives the decay rate and the oscillation frequency of the ladder circuit, are obtained by putting the denominator zero as the solution of the following equations,

for the normal mode,

$$s^2 + s \left[\frac{r}{L_n} + \frac{2}{\rho C_n} \cos^2 \frac{k\pi}{2N} \right] + 2 \frac{(r+\rho)}{\rho LC_n} \cos^2 \left[\frac{k\pi}{2N} \right] = 0. \quad (3-9)$$

For the common mode,

$$s^2 + s \left[\frac{r}{L_c} + \frac{2}{\rho C_c} \cos^2 \left[\frac{(2k+1)\pi}{4N} \right] \right] + 2 \frac{(r+\rho)}{\rho L C_c} \cos^2 \left[\frac{(2k+1)\pi}{4N} \right] = 0 . \quad (3-10)$$

Defining the solutions of above equations as,

$$s_{kn} = -\frac{1}{\tau_{kn}} \pm j\Omega_{kn} \quad (3-11)$$

$$s_{kc} = -\frac{1}{\tau_{kc}} \pm j\Omega_{kc} \quad (3-12)$$

one has,

$$\Omega_{kn} = \sqrt{\frac{2}{L_n C_n} \frac{[\rho+r]}{\rho} \cos^2 \left[\frac{k\pi}{2N} \right] - \frac{1}{4} \left[\frac{2}{\rho C_n} \cos^2 \left[\frac{k\pi}{2N} \right] + \frac{r}{L_n} \right]^2} \quad (3-13)$$

$$\Omega_{kc} = \sqrt{\frac{2}{L_c C_c} \frac{[\rho+r]}{\rho} \cos^2 \left[\frac{2k+1}{4N} \pi \right] - \frac{1}{4} \left[\frac{2}{\rho C_c} \cos^2 \left[\frac{2k+1}{4N} \pi \right] + \frac{r}{L_c} \right]^2} \quad (3-14)$$

Definition of L_n , C_n , L_c and C_c are given in eqs. (2-28) to (2-32).

Resistor r can be neglected in many cases, and one has simpler equations as follows,

$$\Omega_{kn} = \left[\sqrt{\frac{2}{L_n C_n} \cos \left[\frac{k\pi}{2N} \right]} \right] \sqrt{1 - \frac{1}{2\rho^2} \frac{L_n}{C_n} \cos^2 \left[\frac{k\pi}{2N} \right]} \quad (3-15)$$

$$\Omega_{kc} = \left[\sqrt{\frac{2}{L_c C_c} \cos \left[\frac{2k+1}{4N} \pi \right]} \right] \sqrt{1 - \frac{1}{2\rho^2} \frac{L_c}{C_c} \cos^2 \left[\frac{2k+1}{4N} \pi \right]} \quad (3-16)$$

Eqs.(3-15) and (3-16) show dispersion relations of the resonance frequency by sine and cosine functions when a self resistance of the excitation coil is neglected. Installation of the bridge resistor ρ in parallel to the coil shifts the resonant frequency. There exists an equivalent parallel resistor due to AC losses of the magnet in case the bridge resistor is not installed. The lowest resonant frequency is of a primary interest, where $m=1$ for the normal mode and $m=0$ for the common mode. In either case, the resonant frequency is lowered by the addition of the bridge resistor. As is given by eq.(2-35), the characteristic impedance of the magnet string is roughly equal to the characteristic impedance of the transmission line circuit, which is $\sqrt{L/(2C)}$,

the choice of $\rho=Z_{0p}$ gives the zero resonance frequency for $k=0$. It is shown that for the low resonance frequency, to suppress the resonance, the resistance ρ must be lowered according to the dispersion. Bridge resistance of the dispersion relation is plotted in Figures 22 and 23.

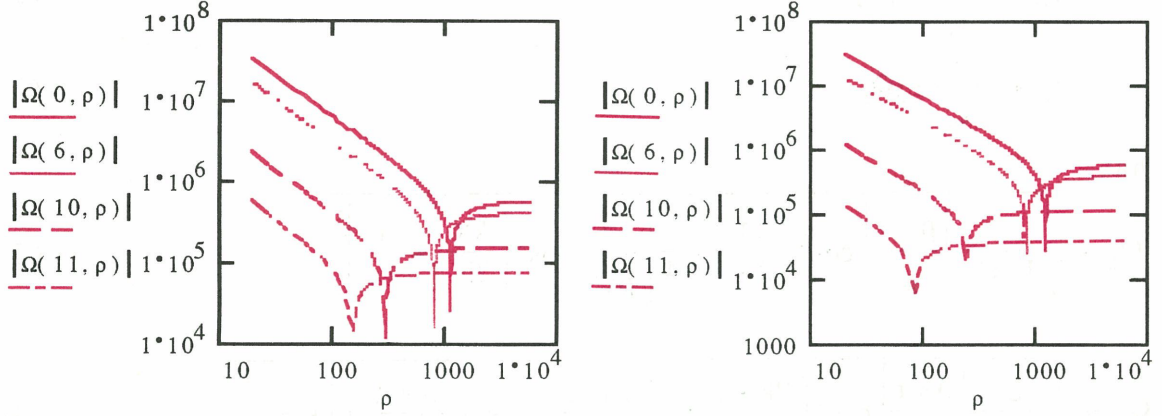


FIGURE 22 and 23. Bridge resistor dependence of the normal mode(left) and common mode(right) resonant frequency for $k=0,6,10$ and 11 .

For the normal mode and the common mode, the attenuation parameter $1/\tau_{kp}$ are,

$$\frac{1}{\tau_{kn}} = \frac{r}{2L_n} + \frac{1}{\rho C_n} \cos^2 \left[\frac{k\pi}{2N} \right] \quad (3-17)$$

$$\frac{1}{\tau_{kc}} = \frac{r}{2L_c} + \frac{1}{\rho C_c} \cos^2 \left[\frac{(2k+1)\pi}{4N} \right]. \quad (3-18)$$

In the above discussion, we obtained following type of equation,

$$\frac{1}{1 + Z_{mp} Y_{mp} + \cos(\zeta_{mp})} = \frac{1}{\rho C_p} \frac{s + \frac{r + \rho}{L_p}}{\left[s + \frac{1}{\tau_{kp}} \right]^2 + \Omega_{kp}^2}.$$

Recalling the inverse Laplace transformation of the above equation[18], the time response to the unit step voltage is written as,

$$\frac{1}{\rho C_p} \left[e^{-\frac{t}{\tau_{kp}}} \left[\cos \Omega_{kp} t + \left[\frac{r + \rho}{L_p} - \frac{1}{\tau_{kp}} \right] \frac{\sin [\Omega_{kp} t]}{\Omega_{kp}} \right] \right].$$

When $\Omega_{kp} < 0$, the time response is not oscillatory. One can still use the above equation by rewriting the above equation with hyperbolic function

using the relation of $\cos(jx)=\cosh(x)$ and $\sin(jx)=j \sinh(x)$. Even when $\Omega_{kp} = 0$, the above equation still holds by taking the limit of $\Omega_{kp} = 0$, which can be written as,

$$\frac{1}{\rho C_p} \left[e^{-\frac{t}{\tau_{kp}}} \left[1 + \left[\frac{r+\rho}{L_p} - \frac{1}{\tau_{kp}} \right] t \right] \right].$$

Ω_{kp} is the angular resonant frequency of the ladder circuit in frequency domain. When the bridge resistor is installed to the magnet coil, the resonant frequencies is decreased with smaller resistance. Criterion for the condition of $\Omega_{kp}=0$ depends on the frequency and written as, for the normal mode,

$$\rho(k) = \sqrt{\frac{L_n}{2C_n}} \cos \left[\frac{k\pi}{2N} \right], \quad (3-19)$$

for the common mode,

$$\rho(k) = \sqrt{\frac{L_c}{2C_c}} \cos \frac{[2k+1]\pi}{4N}. \quad (3-20)$$

To the change of unit step function input voltage, the excitation current of the normal mode $i_n(t)$ and the common mode $i_c(t)$ at the input of the magnet string are in presence of the parallel resistor ρ , which may be either an external bridge resistor or equivalent resistor,

$$i_n(t) = \delta(t) + \frac{2}{\rho N} \sum_{k=0}^{N-1} \left[\cos^2 \left[\frac{k\pi}{2N} \right] e^{-\frac{t}{\tau_{kn}}} \left[\cos \Omega_{kn} t + \left[\frac{r+\rho}{L_n} - \frac{1}{\tau_{kn}} \right] \frac{\sin \Omega_{kn} t}{\Omega_{kn}} \right] \right]. \quad (3-21)$$

$$i_c(t) = \delta(t) + \frac{2}{\rho N} \sum_{k=0}^N \left[\cos^2 \left[\frac{[2k+1]\pi}{4N} \right] e^{-\frac{t}{\tau_{kc}}} \left[\cos \Omega_{kc} t + \left[\frac{r+\rho}{L_c} - \frac{1}{\tau_{kc}} \right] \frac{\sin \Omega_{kc} t}{\Omega_{kc}} \right] \right]. \quad (3-22)$$

δ function appears both in the normal and the common mode current. For simplicity, this plot is omitted in subsequent figures.

Eqs(3-21) and (3-22) are valid for the cable current of general magnet string of the synchrotron. For the HIMAC, where the equivalent bridge resistance of $\rho=6 \text{ k}\Omega$ and the stray capacitance is 1.8 nF , the calculated spike current of

the Quadrupole is shown in Figure 24 and 25 for the normal and the common mode. Typical example of different time scale are shown. Fast spike of tens of kHz is seen. Slow response of the normal mode is the response to the inductance and the series resistance of the magnet.

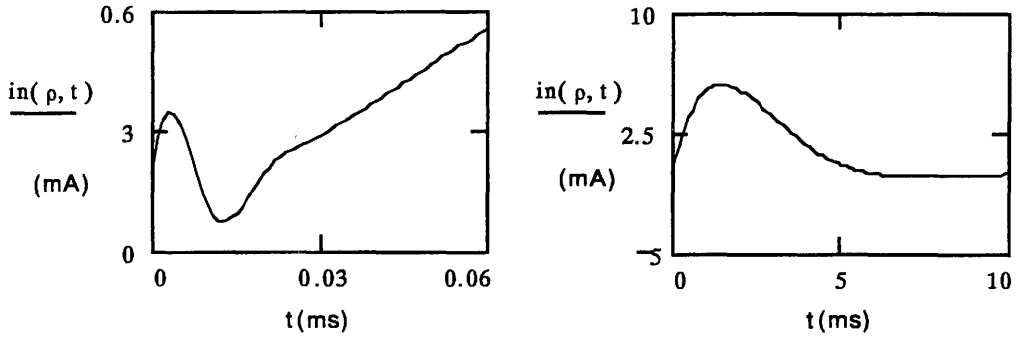


FIGURE 24. Normal mode spike current without the bridge resistor. Equivalent bridge resistor is taken into account.

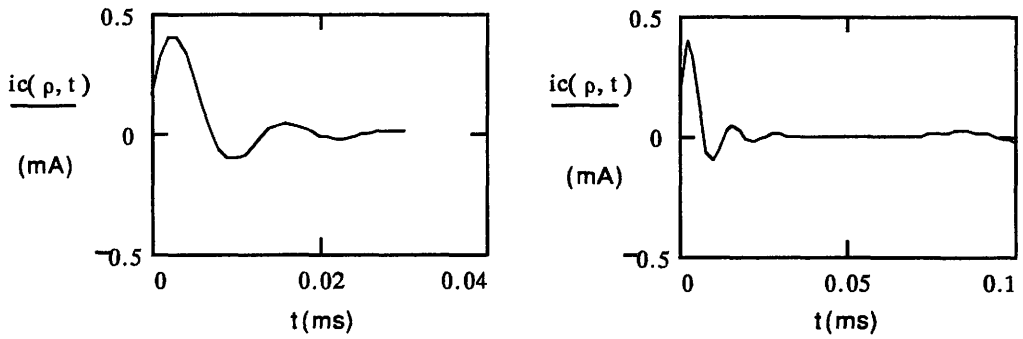


FIGURE 25. Common mode spike current without the bridge resistor. Equivalent bridge resistor is taken into account.

With bridge resistor the current is not oscillatory and the eqs. (3-21) and (3-22) can be approximately expressed as,

$$i_n(t) = \delta(t) + \frac{1}{rN} \left[\left[1 + \frac{r}{\rho} \right] - e^{-\frac{r}{L_n}t} \right] + \frac{2}{\rho N} \sum_{k=1}^{N-1} \cos^2 \left[\frac{k\pi}{2N} \right] e^{-\frac{2t}{\rho C_n} \cos^2 \left[\frac{k\pi}{2N} \right]} \quad (3-23)$$

$$i_c(t) = \delta(t) + \frac{2}{\rho N} \sum_{k=0}^{N-1} \cos^2 \left[\frac{[2k+1]\pi}{4N} \right] e^{-\frac{2t}{\rho C_c} \cos^2 \left[\frac{[2k+1]\pi}{4N} \right]} \quad (3-24)$$

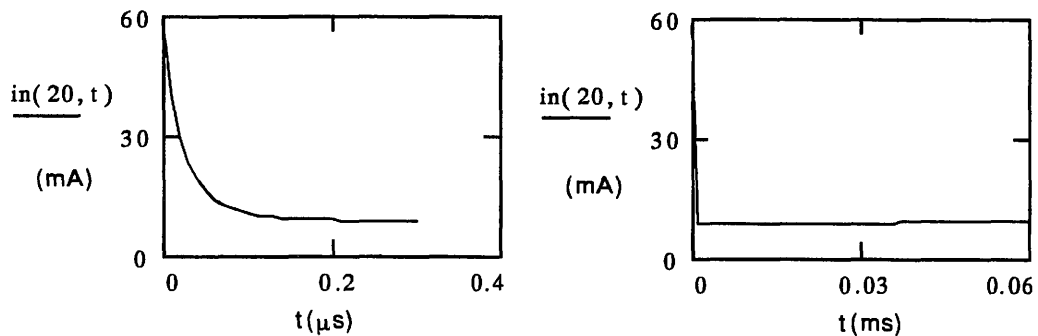


FIGURE 26. Normal mode spike current with bridge resistor of $\rho=20 \Omega$.

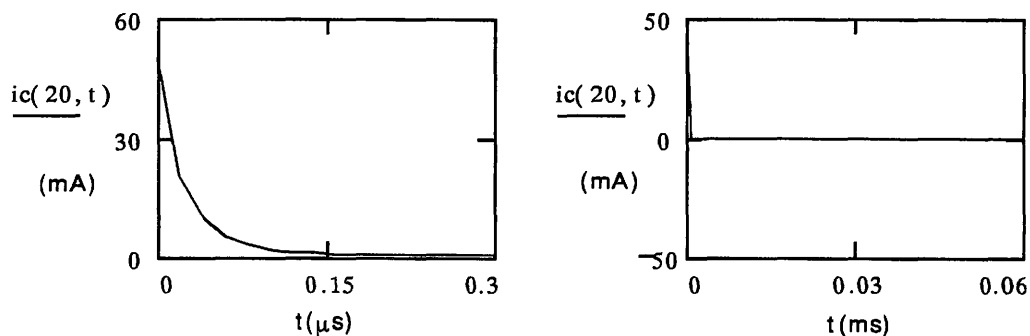


FIGURE 27. Common mode spike current with bridge resistor of $\rho=20 \Omega$.

When the magnitude of the parallel resistance is less than the critical value given by (3-19) and (3-20), the spike current become decaying current. Decaying time constant is inversely proportional to the magnitude of the bridge resistor and the width of the spike becomes much narrower with a sacrifice of larger magnitude as shown in Figures 26 and 27. Calculated spike width is less than μ second. In such a short pulse, a permeability of the magnet core will be close to unity, and the magnet will not respond. Response to δ function and ramp change of the voltage is obtained simply by multiplying 1 or $1/s^2$ to the admittance respectively. Mode currents in any location of the magnet string could be derived in a similar way. Resonance characteristic of them depends upon the location of the coil; the closer the location of the power supply the more the number of resonances, the further from the location of the power supply the fewer the number of the resonances. So far the formulation is performed for even number of cells. Similar formulation holds for the odd number of cells.

IV. Resonance in Power Supply and Magnet String

As discussed in the preceding chapters, the magnet string has resonance characteristics. The power supply is a voltage source and consists of a reactor and capacitor of the mode filter and has a leakage inductance and a stray capacitance. They constitute resonant elements in the power supply. The resonance between the power supply and the magnet string is unavoidable unless cares are taken.

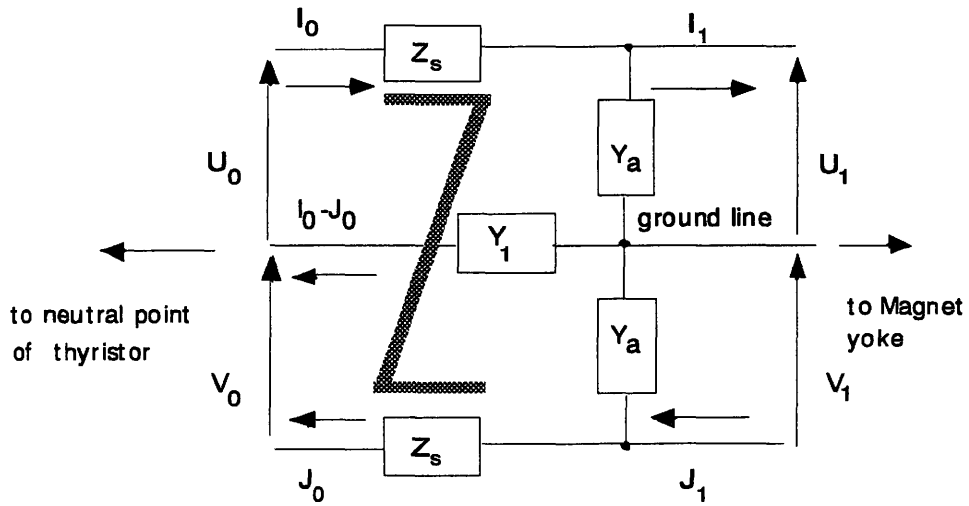


FIGURE 28. Six terminal filter circuit with the HIMAC magnet string.

(i) Symmetric Mode Filter and Earthing of the Thyristor Bank

Ripple or the abrupt change of the voltage goes through the mode filter. Total admittance of the ladder circuit is taken into account in this section. Applying Kirchhoff law in six terminal symmetric low pass filter shown in the Figure, one can derive following equations,

$$G_n \equiv \frac{U_1 + V_1}{U_0 + V_0} = \frac{1}{[1 + [Z_s + Z_M][Y_a + Y_{0n} \coth [N\zeta_{mm}]]]}, \quad (4-1)$$

$$G_c \equiv \frac{U_1 - V_1}{U_0 - V_0} = \frac{1}{\left[1 + 2 \frac{Y_a}{Y_1} + [Z_s - Z_M][Y_a + Y_{0c} \tanh [N\zeta_{mc}]]\right]}, \quad (4-2)$$

where Y_1 and Y_a are the admittance of the neutral point of the thyristor bank and that of the lowpass filter respectively. Above equation is useful to describe the ripple current in the magnet string when the magnitude of the

ripple voltage of the thyristor bank is known.

The admittance of the magnet string appears in the denominator of the transfer function as $Y_{n0} \coth(N\zeta_{mn})$ for normal mode and $Y_{c0} \tanh(N\zeta_{mc})$ common mode. Although the form of the admittance of the normal mode and the common mode is slightly different and show the resonant property, the magnitude is still suppressed mainly by the intrinsic low pass filter term. It will be useful to derive equations of the input admittance \mathcal{Y}_{pt} of the low pass symmetric filter including the magnet string seen from the power supply side,

$$\mathcal{Y}_a = \frac{I_0 + J_0}{U_0 + V_0} = \frac{Y_a + Y_{n0} \coth[N\zeta_{mn}]}{\left[1 + [Z_s + Z_M] [Y_a + Y_{n0} \coth[N\zeta_{mn}]]\right]} \quad (4-3)$$

$$\mathcal{Y}_a = \frac{I_0 - J_0}{U_0 - V_0} = \frac{Y_a + Y_{c0} \tanh[N\zeta_{mc}]}{\left[1 + 2 \frac{Y_a}{Y_1} + [Z_s - Z_M] [Y_a + Y_{c0} \tanh[N\zeta_{mc}]]\right]} \quad (4-4)$$

In case of grounded neutral thyristor bank, the admittance Y_1 is infinite, $Y_a/Y_1=0$. Then, the form of the normal and the common mode admittance becomes similar except the effect of the magnet load. The assumption of the infinite impedance of the magnet load leads to the formula given by Praeg [18]. The common mode admittance of the conventional configuration can be expressed by eq.(4-4) by putting $Z_M=0$ and by reinterpreting Y_a as stray capacitance, where Y_1 and Y_a is comparable, $Y_a/Y_1=1$ and does not show the low pass filter characteristic. This is the reason the thyristor spike and ripples are not suppressed in a conventional synchrotron power supply.

Voltage spike is generated when one thyristor is turned off and the other thyristor is turned on at the interval of 1200 Hz at the HIMAC for the normal mode and that of 600 Hz for the common mode. Due to the presence of the stray capacitance between the transformer, the cable and the bus bar to the ground, the resonance could occur in the power supply side as well as in the magnet string. In the HIMAC, the neutral point of the thyristor bank is grounded through the earth line that is also connected to the yoke of the magnet string.

Choice of the earth of the neutral point of the thyristor bank is a characteristic feature in the HIMAC. In most of previous power supplies, this neutral point is isolated from the ground. Although the concept of the common mode in previous synchrotrons is not clear as in the present study,

the thyristor noise generated in the rectifier returns through the (imaginary) earth line. Neutral point of the thyristor and the (imaginary) earth line is connected by the stray capacitance. The lower the magnitude of this capacitance the lower the thyristor spike in the power supply system. The high impedance of the earth line to the thyristor bank blocks the common mode spike. Blocked thyristor spike current, however, needs other routes of lower impedance and returns to the thyristor bank by giving off the spike noise to the surroundings. This explains why the thyristor power supply is known as a noise source of spikes.

Connecting the neutral point to the earth line of the load reduces the impedance of the earth line to the thyristor bank and increases the flow of the spike noise on the return earth line and at the same time confines the spike noise inside the power supply system. This common mode spike is taken care of by the common mode filter installed in the HIMAC.

(ii) Resonance and modulation of the spike by four voltage source

In this section the full expression of the transfer function of the power supply including the magnet string in presence of stray capacitance in the four voltage sources is shown. The simple model circuit of four voltage sources is shown in Figure 29. The stray capacitances from the midpoint from each thyristor bank are expressed as C_1 , C_2 and C_3 . Inductance L_0 is a leakage inductance of the transformer. Due to this difference in the capacitance, the amplitude of the thyristor spike depends upon the spike voltage of the location of the four thyristor banks. This results in the amplitude modulation of the thyristor spike by illogical ripple.

Let again the thyristor spike voltage of the four banks be

$$v_o \text{ (outer), } v_i \text{ (inner), } u_o \text{ (outer), } u_i \text{ (inner),}$$

and that of at the input of the ladder load be U_0 and V_0 . The spike voltages are generated at an ignition timing of 1.2 kHz in case of 24 pulse thyristor system. Pulse width of each spike is short and they contribute to equivalent high frequency ripple. A close look at the amplitude of each spike reveals that their amplitude is modulated. This amplitude modulation is regarded as the source of the equivalent low frequency illogical ripple. Applying the Kirchhoff law we have a following set of equations,

$$I_i - J_i = s w C_1 \tag{5-1}$$

$$I_i - I_o = (-w + u_i - s L_0 I_i) s C_2 \tag{5-2}$$

$$J_i - J_o = (w + v_i - sL_0 J_i) sC_2 \quad (5-3)$$

$$U_o = -w + u_i + u_o - sL_0 (I_i + I_o) \quad (5-4)$$

$$V_o = w + v_i + v_o - sL_0 (J_i + J_o) \quad (5-5)$$

$$I_o + J_o = [sC_3 + \mathcal{Y}_{io}] [U_o + V_o] \quad (5-6)$$

$$I_o - J_o = [sC_3 + \mathcal{Y}_{io}] [U_o - V_o]. \quad (5-7)$$

Eliminating the common voltage w of the neutral point, the outer and inner currents in the thyristor I_o, I_i, J_i, J_o and the corresponding voltage v_o, v_i, u_o, u_i , one obtains following equations for the normal mode voltage ($U_o + V_o$) and the common mode voltage ($U_o - V_o$) expressed by $(u_i + v_i), (u_o + v_o), (u_i - v_i)$ and $(u_o - v_o)$,

$$[1 + s^2 L_0 C_2 + sL_0 [2 + s^2 L_0 C_2] [\mathcal{Y}_{io} + sC_3]] [U_o + V_o] = [u_i + v_i] + [1 + s^2 L_0 C_2] [u_o + v_o] \quad (5-8)$$

$$\left[1 + s^2 L_0 C_2 + 2 \frac{C_2}{C_1} + sL_0 [\mathcal{Y}_{io} + sC_3] \left[2 + \frac{2}{s^2 C_1 L_0} + s^2 L_0 C_2 + 2 \frac{C_2}{C_1} \right] \right] [U_o - V_o] \\ = [u_i - v_i] + \left[1 + s^2 L_0 C_2 + 2 \frac{C_2}{C_1} \right] [u_o - v_o] \quad (5-9)$$

where \mathcal{Y}_{nl} and \mathcal{Y}_{cl} are the normal and the common mode admittance of the ladder circuit given by eqs.(4-3) and (4-4). \mathcal{Y}_{nl} and \mathcal{Y}_{cl} show resonance as are shown in previous chapters. These equations give a transfer function of the voltage from the thyristor of the four voltage sources to the entrance of the low pass filter. The important lessons from the equations are;

- (i) transfer function of the common mode and the normal mode are different,
- (ii) transfer function of the thyristor of the inner bank and the outer bank is different,
- (iii) there is a mechanism of the enhancement of the resonance where the residue is given by equating the coefficient of the left-hand side of equations to zero.

Examination of the equations reveals that the difference between the modes appears as terms multiplied by a factor $2C_2/C_1$ as found in the previous chapter and again earthing the midpoint of the thyristor bank makes two equations similar. This can be understood that in general the impedance at the ground line appears only in the equation of the common mode whereas the impedance at the P and N lines appears in both equations. When the mid-point is grounded, the equation for the common mode is thus given by,

$$[1 + s^2 L_0 C_2 + s L_0 [2 + s^2 L_0 C_2] [\mathcal{Y}_{1e} + s C_3]] (U_0 - V_0) = [u_i - v_i] + [1 + s^2 L_0 C_2] [u_o - v_o] \quad (5-10)$$

The equation of the normal and the common mode voltage is the same except the admittance of the ladder circuit. Further elaborate model such as the one incorporating a snubber circuit is possible. It is, however, the essential property of the existence of the resonance and unified treatment of the normal and the common mode remains unchanged.

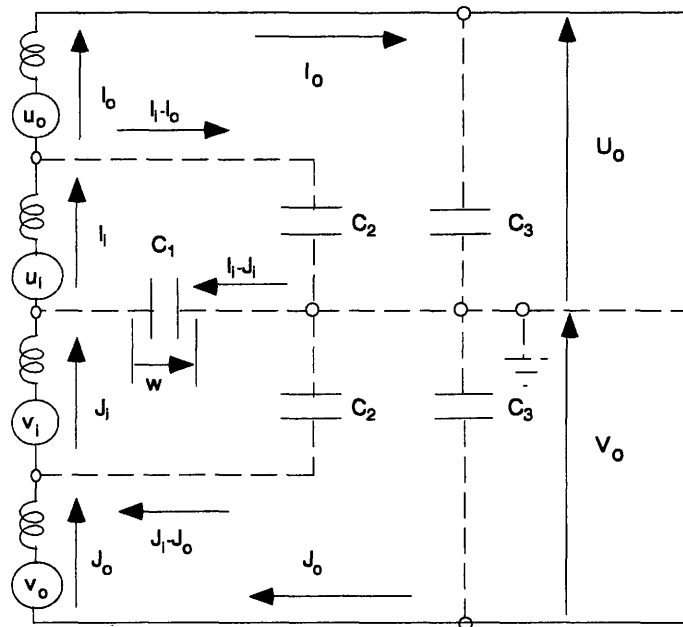


FIGURE 29. Block diagram of the power supply in front of the low pass filter. The dotted lines show virtual lines of the stray capacitances and the virtual ground line. In most of the power supplies, the thyristor is floated and C_1 has finite magnitude where in the HIMAC, the thyristor bank is grounded.

V. Conclusion

By finding the importance of the common mode besides the normal mode, we could make a formulation of the normal and common mode in the power supply and the magnet string. Six terminal ladder circuit found out to be decomposed into two set of four terminal circuit of two different modes. When a degree of symmetry of the circuit with respect to the earth is high, two modes become a decoupled normal and common mode. Quantities of the voltage, current, admittance can be expressed in simple analytical expression as a complex number. Frequency domain as well as time domain solution is

available. The role of the bridge resistor was evaluated by simple expression in a closed form. Performance of the mode filter, the normal and the common mode filter, was evaluated in a presence of elements of resonant property. The effect of the separate connection of the coil is evaluated by the change of the common mode impedance. Analysis based upon the formulation supports the performance of the small ripple content of the HIMAC synchrotron and will be useful for other synchrotrons. In the HIMAC, logical ripples of the power supply is eliminated in this way. Normal mode 50 Hz and 100 Hz can be eliminated by other standard method. Owing to the common earth line of the power supply and the load that is introduced from the property of the "symmetry", the whole system can be "noiseless" seen from outside the power supply as the noise current is confined inside the power supply. The symmetry can provide the decoupling of individual systems such as the low level power supply of the control circuit. If this method is applied to the power supply of other synchrotron, high performance as the HIMAC will be obtained.

VI. Acknowledgement

The author expresses their thanks to Director General Y. Hirao, Director K.Kawachi for their continuing support and encouragement. This paper will not be completed without a patient guidance and discussions with prof.K. Sato of University of Osaka and Prof.S.Matsumoto of Dokkyo Medical University. Discussions are benefited with the member of the HIMAC, Drs. K.Noda, E.Takada, S.Yamada, M.Kanazawa, A.Itano. The author also likes to thank to collaborators during a construction of the HIMAC, such as Drs. Y. Irie, S.Watanabe, H.Sato, T.Sueno of INS and KEK. This work will not be completed without a cooperation of Physics and Engineering Division Group. The author thanks to Drs.T.Tomitani of Physics Division and T.Aoki of AEC for valuable comments. The discussion with H.Kubo of Hitachi who manufactured the system was inevitable. The author thanks Dr. H.Bicshel of NPL, University of Washington and S.D.Whitehead for revising the manuscript.

VII. References

- [1]M.Kumada et al., "The HIMAC Very Low Ripple Synchrotron", EPAC, 1994.
- [2]M.Kumada,"Synchrotron Power supply of sub-ppm Ripple Current", submitted to Particle Accelerator.
- [3]M.Kumada et al.,"Recent improvement of HIMAC synchrotron", 10 th Symp. On Accelerator and Technology,1995, Hitachi Naka.
- [4]E.Regenstreif,"The CERN proton synchrotron",CERN 59-29, pp.153-158.
- [5]Van Der Meer,"Delay line effects in the 300 GeV magnet circuit", ISR-PO/S., MC/12, October 22,1969.
- [6]M.Kumada et al.,"System design of main magnet power supplies of the HIMAC heavy ion synchrotron", The 8th Symp. on Accelerator and Technology, 1991, Saitama, Japan, pp.199-201.
- [7]M.Kumada, "Design of the HIMAC Synchrotron Power Supply", PAC93, Washington DC, pp.1291-1293.
- [8]M.Kumada et al.,"Analysis of the HIMAC synchrotron power supply", The 9th Symp. on Accelerator and Technology, 1993, KEK, pp.211-213.
- [9]R.E.Shafer,"Eddy currents, dispersion relations and transient effects in superconducting magnet", IEEE Transaction on magnets, Vol.MAG-17, No.1, January,1981, pp.722-725.
- [10]R.E.Schafer,"Transmission line property of long strings of superconducting magnets", IEEE Vol.MAG-17, NO.1, Jan.,1981, pp. 726-727.
- [11]K.M.Smedley,R.E.Shafer,"Measurement of AC electrical characteristics of SSC superconducting dipole magnets", pp. 629-631.
- [12]R.E.Schafer, K.M Smedley, "Electrical characteristics of long strings of SSC superconducting dipoles", HEACC'92, HAMBURG, pp.298-300.
- [13]O.Calvo,G.tool,"Analysis of transmission line effects in the SSC magnet system", Fermilab, CH 2387-9/87/0000-1425,1987 IEEE, Particle accelerator conference, Washington D.C., pp.1425-1427.
- [14]H.J.Eckoldt,"Simulation of transmission line effects within an octant of the superconducting HERA ring during an energy ramp",DESY,HEACC'92 HAMBURG, pp.329-331.
- [15]R.Bacher,K.H.Mess,M.Seidel,"Transmission line characteristics of the S.C. HERA dipole and Quadrupole string", HEACC'92, HAMBURG, pp.301-303.
- [16]M.Kumada,"Mode Analysis of Synchrotron magnet strings", to be published in the proceedings of Particle Accelerator Conference,PAC95, Dalas.
- [17]M.Kumada,"Mode Mixing in Synchrotron Magnet Power Supply",

submitted for publication.

[18]W.Praeg,"A high-current low-pass filter for magnet power supply", IEEE transactions on industrial electronics and control instrumentation, Vol.IECI-17. N0.1, February,1970, pp.16-22.

[19]Y.Ohno,"Theory of modern transient phenomena", (in Japanese), Ohm publishing,1994, pp.107-110.

[20]S.Moriguchi et al.,"Formula in Mathematics II", Iwanami publishing, p.21.

[21]Mathcad, Mathsoft Inc.,201 Broadway, Cambridge, Ma.,02139,USA

[22]S.C.Snowdon,"Transfer function between magnetic field and excitation current in Main ring bending magnets", FNAL Internal Report,TM-325,1971.

Appendix. Decomposition of Partial Fractional Expression

(i) Expansion theorem

Derivation of the equations of (3-6) and (3-7) from the equations of (3-3) and (3-4) is a consequence of the expansion theorem. We will prove this by the mathematical induction. Consider a rational fractional expression of $Q(s)$,

$$Q(s) \equiv q_1(s) \equiv \frac{\prod_{k=1}^N (x + b_k)}{\prod_{k=1}^N (x + a_k)} \quad (\text{A-1})$$

We assume $Q(s)$ can be expressed by a partial fraction expression for $k=N$ as,

$$Q(x) \equiv q_2(x) \equiv 1 + \sum_{k=1}^N \frac{c_k}{x + a_k} \quad (\text{A-2})$$

with a condition that,

$$a_i \neq b_j \text{ and } a_i \neq a_j \text{ for } i=1,2,\dots,N \text{ and } j=1,2,\dots,N.$$

(1) For $N=1$

$$q_1(x) = \frac{x + b_1}{x + a_1} \text{ and } q_2(x) = 1 + \frac{c_1}{x + a_1} = 1 + \frac{b_1 - a_1}{x + a_1} = q_1(x) \quad (\text{A-3})$$

(2) Assuming the equality of $q_1(x)=q_2(x)$ for $N=n$, we have

$$\begin{aligned} q_1(x) = Q_{n+1}(x) = Q_n(x) \left[\frac{x + b_{n+1}}{x + a_{n+1}} \right] &= \left[1 + \sum_{k=1}^n \frac{c_k}{x + a_k} \right] \left[\frac{x + b_{n+1}}{x + a_{n+1}} \right] \\ &= 1 + \sum_{k=1}^n c_k \left[\frac{b_{n+1} - a_k}{a_{n+1} - a_k} \right] \frac{1}{x + a_k} + \frac{[b_{n+1} - a_{n+1}]}{x + a_{n+1}} \left[1 - \sum_{k=1}^n \frac{c_k}{a_{n+1} - a_k} \right] \\ &\equiv 1 + \sum_{k=1}^{n+1} \frac{d_k}{x + a_k} = q_2(x). \end{aligned} \quad (\text{A-4})$$

Similarly, we can write a rational function $Q(s)$ of the Laplace operator s can

be written as[19],

$$Q(s) = P(s) + \frac{N(s)}{D(s)} \quad (A-5)$$

where $P(s)$, $N(s)$ and $D(s)$ are polynomial in "s" with the condition that the order of $D(s)$ is at least one higher than the order of $N(s)$.

Furthermore if $D(s)$ can be written as,

$$D(s) = (s - s_1)(s - s_2)(s - s_3) \dots (s - s_N) \quad (A-6)$$

then one has,

$$Q(s) = \sum_{i=1}^N \frac{A_i}{s - s_i}, \quad \text{with} \quad A_i = N(\alpha) \left[\frac{dD}{ds} \Big|_{s_i = \alpha} \right]^{-1}. \quad (A-7)$$

This theorem holds for complex number of residual[18]. In our case, the admittance \mathcal{Y}_p is written as,

$$\mathcal{Y}_p = P(X) + \frac{N(X)}{D(X)} \quad (A-9)$$

where X is defined by

$$X = \cosh(\zeta_{mp}(s)) = 1 + Z_{mp}(s)Y_{mp}(s). \quad (A-10)$$

For the proof of the Heaviside expansion theorem, "s" is not necessary to be imaginary number but can be complex number. One can replace "s" by X in the expansion theorem. In the case of the total admittance \mathcal{Y}_p normalized by $Y_{mp}(s)$ the numerator and the denominator have the same order in the power of X and $P(X)$ is 1.

(ii) Derivation of the partial fraction

Let us define a normalized total admittance of the ladder circuit of the common mode as,

$$y_n = \frac{\mathcal{Y}_n}{Y_{mn}} = 1 + \sum_{k=1}^{N-1} \frac{F_k}{\cosh \zeta_{mn} - \cos \frac{k\pi}{N}}. \quad (A-11)$$

We will derive one of the amplitude function factor F_k as an example,

$$\begin{aligned} F_k &= \frac{\sinh(x)}{\cosh(x)} \frac{\cosh(Nx)}{\sinh(Nx)} \Bigg|_{x = \cos \left[\frac{k\pi}{N} \right]} = \frac{\sinh(x)}{[\cosh(x) - 1]} \frac{\cosh(Nx)}{N \cosh(Nx)} \frac{dx}{dX} \Bigg|_{x = \cos \frac{k\pi}{N}} \\ &= \frac{\sinh^2(x)}{(\cosh(x) - 1)} \Bigg|_{x = \cos \frac{k\pi}{N}} = \frac{1 + \cos \left[\frac{k\pi}{N} \right]}{N} = \frac{2 \cos^2 \left[\frac{k\pi}{2N} \right]}{N}. \end{aligned} \quad (A-12)$$